SURFACE-WATER HYDROLOGY OF PROPOSED TEXAS LOW-LEVEL RADIOACTIVE WASTE ISOLATION SITE

M. Saleem Akhter, Joong Hoon Kim, and Alan R. Dutton

Prepared for

Texas Low-Level Radioactive Waste Disposal Authority

under Interagency Contract Number IAC (88-89)-0932

Bureau of Economic Geology

W. L. Fisher, Director

The University of Texas at Austin

Austin, Texas 78713

August 1989

QAe7450

INTRODUCTION

The purpose of surface-water hydrology studies at the proposed low-level radioactive waste isolation site in Hudspeth County, Texas, was to define the flooding potential as interpreted from the applicable regulatory requirements. Federal Emergency Management Agency Report 37 (FEMA, 1985), which details guidelines and specifications for flood insurance studies, and other published reports (Texas Department of Water Resources, 1979a-c) were used as the primary source to develop the scope of field reconnaissance and hydrologic evaluation of the study area. The scope of this project included:

(1) Delineation of drainage basins and identification of drainage divides and potential surface-water pathways on and near the study area.

(2) Collection of rainfall and surface runoff data from the study area.

(3) Development and evaluation of a hydrologic model to determine extent of flooding at the site due to actual and potential storms.

(4) Definition of a 100-yr floodplain for the study area by determining depth, velocity, and extent of surface runoff resulting from a hypothetical 100-yr rain storm.

The approach adopted to meet these objectives consisted of estimating soil properties, monitoring rainfall and surface-water runoff rates, matching simulated flows to observed data on surface-water runoff, and predicting flow characteristics on the basis of calibrated computer models.

Two methods were used to evaluate the flooding potential. The first method treated the study area as an active alluvial fan; that analysis indicates that the study area lies within a 100-yr floodplain. This method excluded the topographic features and the hydraulic storage in the existing channels. The second method incorporated computer models in order to determine flood elevations for a 100-yr flood; this analysis indicates that runoff from such an event would be mostly contained within

the existing channels, leaving large sections in the middle of the study area uninundated.

SITE CHARACTERISTICS, DATA, AND METHODOLOGY

The 100-yr floodplain map published by FEMA for the Hudspeth County area (fig. 1) includes only a narrow strip along the main channels on the basis of a qualitative assessment of possible flow conditions. This report describes a quantitative evaluation of the flooding potential at the site, incorporating measured parameters, detailed mapping of drainage subbasins, and simulation of surface-water flow using several analytic techniques.

Surface Drainage Pattern and Soil Characteristics

The Hudspeth County study area is located on an alluvial plain characterized by gentle slope (1 to 1.5 percent) having dendritic drainage patterns. The area is well vegetated and includes drought-tolerant grasses, cacti, and spiny shrubs. The surface soils consist of coarse gravel and sands (Baumgardner, 1989). Water infiltration properties of the surface soils were assumed to be those of Soil Group "B" according to the USDA Soil Conservation Service classification (Soil Conservation Service, 1975). The study area is located within the watershed of the lower fork of the Alamo Arroyo and the upper fork of the Camp Rice Arroyo (fig. 2). The drainage channels in the study area are not well defined except in the east and southeast parts where channel depths are 1.5 to 2 ft (0.46 to 0.61 m) and widths are 3 to 5 ft (0.91 to 1.52 m). Bed materials in the channels are sand and fine gravel.

Rainfall Data

Rain events in West Texas mostly are localized storms causing high-intensity rainfall in a small area; adjacent subbasins may receive little precipitation. For this

project, the Department of Meteorology, Texas A&M University, compiled historical rainfall data from stations located in Hudspeth and El Paso Counties for the 1859-1989 period. In addition, site-specific rainfall data were gathered at rain gauges installed at four stations in the study area and at one rain gauge on the Diablo Plateau (fig. 2). Rainfall intensity data were developed using various published techniques (Chow and others, 1988). Precipitation data for a 100-yr return frequency storm were calculated by the Department of Meteorology.

Floodplain Models

Rainfall elicits a rapid runoff response in the basin under study: runoff closely follows the onset of rainfall and peaks and recedes rapidly. There is negligible interception and little depression storage, and numerous small channels rapidly carry away the runoff. Absence of well-incised channels indicates overland sheet flow to be the predominant surface-water runoff path.

Two analytic techniques were used: (1) computer modeling with HEC-1 and HEC-2 programs and (2) a FEMA method (also known as the Dawdy method) for analysis of shallow overland flow on alluvial fans. The HEC programs were developed by the U.S. Army Corps of Engineers, Hydrologic Engineering Center in Davis, California. The HEC-1 program is used to determine peak flow (U.S. Army Corps of Engineers, 1981) and the HEC-2 program is used to calculate water-surface profiles during flood flow (U.S. Army Corps of Engineers, 1982). HEC-2 was designed for modeling flow in well-defined channels. Results of modeling overland flow on a relatively flat topography need to be carefully evaluated. The FEMA method calculates the flood height in the lower reaches of active alluvial fans. It uses statistical analysis to relate the probability of given discharges at the apex of a fan to the probability of certain depths and velocity of flow occurring at any point on the fan below the apex. The identification of alluvial fan and flow regimes is critical for

correct application of the FEMA method.

The evaluation of flooding at the study area focused on (1) the drainage basin and subbasins forming the watershed for the Alamo Arroyo and (2) a larger area including the Camp Rice and Alamo Arroyo drainage basins and interarroyo plain. Technical details of these analyses are included in the following sections.

Calculation of Discharges

Calculated discharges are based on digitized water-level records from stream gauging stations 1, 2, and 3 (fig. 2), installed in channels in the study area. One still well was placed in the swale that carries runoff downstream from the southwest corner of the site. Additionally, a total of 28 crest stage gauges were installed in the study area to measure depth of overland sheet flow. A summary of the water levels from the gauging stations and the still well is shown in table 1. Drainage basins delineated for calculation of runoff and the stream gauging stations are shown on figure 2. The water levels at 10-min intervals were read from the water-level versus time record. Then, the base-line water level was subtracted from the gross levels to obtain flood water depths, which were used to calculate discharges. The water-level data recorded at the still well and at the crest stage gauges were not used directly in the surface runoff calculation. However, these data provided a verification of the range of values calculated from the stream-gauge data.

Channel cross sectional area was obtained by surveying. Four different channel cross sections for gauging station 2 were used to calculate hydrographs for each rainfall event. The total cross section in gauging station 2 (fig. 3) included a nearby unpaved road, whereas the partial cross section (fig. 4) did not include the road.

Two other cross sections were 50 and 63 ft (15.2 and 19.2 m) upstream of gauging station 2 (figs. 5 and 6).

Assuming flow in channels to be at steady state, discharge was calculated by Manning's equation (Chow and others, 1988),

$$Q = (1/n)\ A\ R^{2/3}\ S^{1/2} \quad (1)$$

where Q is the discharge (m^3/sec), n is Manning's roughness coefficient, A is the channel cross-sectional area (m^2), P is wetted perimeter (m), R is hydraulic radius (m), which is A/P, and S is friction slope. Five surface-water runoff events that resulted from rainfall on 07-29-88, 08-02-88, 08-09-88, 08-21-88, and 09-02-88 were analyzed for gauging station 2. The calculated discharges for the total and partial cross sections at gauging station 2 are shown in figures 7 through 11.

Gauging station 1 is located where flow from basins II and III were interpreted to converge (fig. 2). A discharge hydrograph of the 07-29-88 rainfall event was calculated for gauging station 1. Observed discharges at gauging station 1 were expected to be larger than those at gauging station 2, where runoff from drainage basin II was measured, because all runoff from drainage basins II and III pass gauging station 1. However, the peak discharge of 4.80 ft^3/sec (0.136 m^3/sec) observed at gauging station 1 is smaller than either the observed peak discharge of 34.7 ft^3/sec (0.98 m^3/sec) for the total cross section (including the road) or the partial cross-section discharge of 136.3 ft^3/sec (3.85 m^3/sec) at gauging station 2. The road passing along the south side of the site appears to channel and divert water from the main stream at gauging station 1. Figure 12 compares observed discharge hydrographs of the 07-29-88 event at gauging stations 1 and 2. Precipitation data from rain gauge 1, which is nearest to gauging station 1, and those from rain gauge 3, which is nearest to gauging station 2 (fig. 2), are also included in figure 12 for comparison.

There were no major rainfall or runoff events between September 15, 1988, and August 1, 1989, the period covered by current data records at gauging station 3.

Modeling with HEC-1

The HEC-1 computer program (Flood Hydrograph Package) was used to simulate the surface runoff at gauging station 2 for the 5 recorded events. Weighted averages of the rainfall data for the 5 rain gauges (fig. 2) were used. Data from Diablo Plateau rainfall gauging station (station 4) were not available for the events of 07-29-88, 08-02-88, and 08-09-88. Rainfall data for the 5 rainfall events are shown in tables 2 through 6.

The loss due to infiltration is calculated in HEC-1 modeling on the basis of specified values of CN and STRTL, where CN is the curve number related to the type of soil group and STRTL is an initial depth of abstraction before ponding. The Soil Conservation Service (SCS), U.S. Department of Agriculture, has related the infiltration loss characteristics of soil groups to curve numbers (CN's) on the basis of empirical data (SCS, 1975).

Parameter Calibration

HEC-1 model parameters were calibrated on the basis of rainfall and runoff data from the study area. Infiltration-loss parameters of initial abstraction (STRTL) and SCS curve number (CN) were optimized for the 5 rainfall events, and the results are summarized in table 7. Also, the optimum initial abstraction (STRTL) and constant-loss rate (CNSTL) were found for the 5 rainfall events, and the results are summarized in table 8. Table 9 shows the percentages of actual rainfall loss for the 5 rainfall events. The hydrographs calculated from the observed water depths were compared with those obtained from HEC-1 with various SCS curve numbers. STRTL value was not specified in the input to allow the HEC-1 program to compute a

default value as a function of a given curve number.

Figures 7 through 11 compare hydrographs of observed total and simulated discharge with various curve numbers for the 5 rainfall events. The time (horizontal) axis represents the time since the rainfall began. The simulated hydrograph based on a curve number of 75 has about the same volume of water as the observed hydrograph, whereas the simulated hydrograph based on a curve number of 73 resulted in a peak discharge similar to the observed peak discharge for the total channel cross section (fig. 7). Because the peak discharge is the critical parameter to match, 73 appears to be the appropriate estimate of curve number for the rainfall event of 07-29-88. Similarly, estimated curve numbers of 90, 90.5, 87, and 87 correspond to the rainfall events of 08-02-88, 08-09-88, 08-21-88, and 09-02-88, respectively. The average curve number is 82. Because the infiltration losses are a function of antecedent moisture conditions (that is, dependent upon the quantity and frequency of rainfall), there is a certain variability in the curve numbers for different events.

The discrepancy (lag) between times of the observed and those of the simulated peak discharges is due to the underestimation of storage in channels, which was necessary in order to accurately match flow volume between observed and simulated discharges. For the purpose of delineating the floodplain, the peak flow is the critical parameter. The discrepancy in peak times is the result of imperfect mathematical description of channel geometry.

Kinematic Wave Routing Model

The HEC-1 program was also used in conjunction with a kinematic wave routing model for surface runoff by dividing the basin for gauging station 2 into 10 subbasins (fig. 13). This exercise allowed an evaluation of the sensitivity of peak discharge to

different flow configurations. This model routes flow through separate channels (collector channels) in the various subbasins using the kinematic interpretation of the equations of motion. Flow in the channels is computed from Manning's equation (1), and movement of the flood wave is described by the continuity equation. In the model, these separate channels then coalesce into a single (main) channel on the downstream end of the basin or watershed. The kinematic wave routing allows a modular approach whereby hydraulic parameters within individual subbasins can be separately specified.

The two rainfall events of 07-29-88 and 08-21-88 were analyzed by the kinematic wave routing model. The other events were too small to be analyzed. Figures 14 and 15 compare the observed and the simulated hydrographs obtained by kinematic routing with various curve numbers. From the figures it was concluded that curve numbers of 78 and 90 were appropriate for the events of 07-29-88 and 08-21-88, respectively. The simulated hydrographs reflect a lag time for the peak discharge relative to the observed hydrographs. This phenomenon probably is a result of the storage in the various channels within the subbasins, which delays the arrival of the peak discharge.

Modeling of 100-yr and Probable Maximum Floods

The average CN value of 82 from table 7 was used as the loss parameter in the 100-yr flood and Probable Maximum Precipitation (PMP) analyses. STRTL values were not specified in the input because the best-fit values of STRTL vary from 4 to 20 (table 6). The HEC-1 program computes default values as a function of given curve numbers. The parameters in Table 8 that were calculated with the uniform loss-rate option in HEC-1 modeling were not used in the analysis because of their large variations.

The intensity and temporal distributions of rainfall used in this study were patterned after the methodologies used in studies of flooding in El Paso, Texas (Espey Huston & Associates, Inc., 1981; Frederick and others, 1977; Miller and others, 1984). A correction factor was applied to increase the rainfall volume in the study area slightly. Table 10 shows the 5-min-interval rainfall distributions used in this study for both the 100-yr frequency rainfall and the probable maximum precipitation.

Alluvial Fan Method

Another methodology used in this study is based on procedures developed by Dawdy FEMA, 1985) to estimate flood height in the lower reaches of active alluvial fans. It makes use of statistical analyses that relate the probability of given discharges at the apex of a fan to the probability of certain depths and velocity of flow occurring at any point on the fan below the apex (FEMA, 1985).

Identification of Flow Regime

The flow regime on an alluvial fan during a major flood event depends on the number of channels created by the flow of water. At peak flow during a major flood event on an active fan, water does not spread evenly over the fan but is confined to intrafan channels that carry the water from the apex to the toe of the fan. These channels are found to occur in three patterns, namely, single channel, split channel, and braided channel (fig. 16). The single channel is located just below the mouth of the canyon in the upper region of the fan, and it is formed by erosion of the loose material that composes the fan. The split and multiple channels are formed through repeated bifurcation of channels below the apex of the fan that finally terminate in a braided sheet flow channel. The single channel region is defined by the length of the

single channel measured from the mouth of the canyon to the point where the flood channel splits; this length decreases with the ratio of canyon slope to fan slope.

To apply the alluvial-fan flooding method, the concept of a single equivalent channel is used to compute flood depths. For the purpose of flood mapping, the computed depth of water flow on alluvial fans is the depth of flow (depth of channel) in the channel that carries a given discharge to the toe of the fan surface. Water depths between 0.5 and 1.5 ft were rounded to 1 ft, which is a FEMA criterion for delineating a flood zone.

The length of the single channel can be determined using figure A5-1 of the FEMA 37 report. The ratio of canyon slope to fan slope was determined from a topographic map of the study area (fig. 17), and this ratio (2.15) indicated that no single channel region was present on the site. Therefore, the procedure for a multiple channel region was applied for determination of flood height.

Determination of Flood Discharge-Frequency Distribution

A complete flood discharge-frequency distribution is required to determine the source of flooding at the apex of each alluvial fan using Log-Pearson Type III analyses in accordance with the guidelines for determining flood flow frequency (Riggs and others, 1968; U.S. Department of Interior, 1982). Because the data for those analyses were not available for the site, flows of various recurrence intervals were computed from HEC-1, and the following synthetic Log-Pearson Type III parameters were estimated:

$$Q_{.01} = 3570 \text{ cfs}, \quad Q_{.10} = 2706 \text{ cfs}, \quad Q_{.50} = 941 \text{ cfs}$$

where $Q_{.01}$, $Q_{.10}$, and $Q_{.50}$ are discharges with 0.01, 0.10, and 0.50 exceedance probabilities, respectively.

the skew coefficient,

$$G = -2.50 + 3.12\ [\log(Q_{.01}/Q_{.10})/\log(Q_{.10}/Q_{.50})] \quad (2)$$
$$= -1.682,$$

standard deviation,

$$S = [\log(Q_{.01}/Q_{.50})/(K_{.01}-K_{.50})] \quad (3)$$
$$= 0.654,$$

and the mean of logarithms,

$$X = \log(Q_{.50}) - K_{.50}\ S \quad (4)$$
$$= 2.80,$$

where $K_{.01}$ and $K_{.50}$ are the number of standard deviations above and below the mean for the Pearson Type III exceedance probabilities of 0.01 and 0.50 and skew coefficient G.

Since the skew coefficient was not zero, the following transformation variables were computed:

$$m = X - 2S/G = 3.578 \quad (5)$$

$$\alpha = 2/GS = -1.819 \quad (6)$$

$$\lambda = 4/G^2 = 1.416 \quad (7)$$

$$a = \alpha - 0.92 = -2.739 \quad (8)$$

The transformation constant was computed as

$$C = (\alpha/a)\ \lambda\ \exp(0.92m) = 25.29 \quad (9)$$

The Log-Pearson Type III parameters were transformed using the variables computed above according to the following equations:

$$Z = m + \lambda/a = 3.061 \quad (10)$$

$$S_z^2 = \lambda/a^2 = 0.189 \quad (11)$$

$$S_z = 0.434 \quad (12)$$

$$G_z = 2/\lambda^{1/2} = 1.681 \quad (13)$$

Determination of Discharge for 0.5-ft Flood Depth

As determined in the section on identification of flow regime, there is no single channel region on the site. Therefore, the procedure for a multiple channel region was applied. For the fan slope $S_f = 0.013$ and Manning's coefficient $n = 0.04$, the discharge Q (cfs) that corresponds to the depth $D = 0.5$ (ft) was calculated by iteratively solving the following equation:

$$D = 0.0917\ n^{.6}\ S_f^{-.3}\ Q^{.36} + 0.001426\ n^{-1.2}\ S_f^{.6}\ Q^{.48} \quad (14)$$

For $D = 0.5$ ft, Q was found to be 380 cfs.

Determination of Fan Width at 0.5-ft-Depth Boundary

The Log-Pearson Type III standard deviation above and below the mean frequency was computed for the discharge that corresponds to 0.5 ft depth zone boundary using equation 15:

$$K = (\log Q - Z)/S_z = (\log 380 - 3.061)/0.434 = -1.109 \quad (15)$$

Then the probability of occurrence of the discharge for the depth was

$$P\ (Q > 380) = P\ (K > -1.109) = 0.866 \quad (16)$$

The fan arc width was computed as

$$W = 3610\ A\ C\ P = 3610 \times 1.5 \times 25.29 \times 0.866 = 118{,}600 \text{ ft.} \quad (17)$$

where A is the avulsion coefficient (factor accounting for the possibility of channel switching during major floods on active alluvial fans), and C is the transformation constant. Assuming a constant expansion angle, the 100-yr flood based on the alluvial fan model would reach an arc width of 118,600 ft far downstream from the location of the study area (fig. 17).

Analysis with HEC-2

The HEC-2 computer program calculates water-surface profiles in natural or man-made channels. The program is also designed for application in floodplain management and flood insurance studies to designate flood hazard zones.

A HEC-2 run was implemented for Channel B (drainage basin II, fig. 2) using a 100-yr-frequency peak discharge of 8,500 cfs, which was calculated for the channel by HEC-1. Nine channel cross sections were selected (fig. 18). HEC-2 results indicate that the upstream parts (cross sections 8 and 9) of Channel B could not convey more than 4,000 cfs. Extra discharge was likely to diverge into nearby Channel C, which had greater conveyance. A peak discharge of 4,000 cfs was obtained by HEC-1 for the Drainage Basin III, which includes Channel C (fig. 18). A discharge of 8,500 cfs, therefore, was used in the HEC-2 simulation for Channel C because the extra discharge of 4,500 cfs from Channel B was expected to diverge into Channel C. Channel C was found to have adequate capacity to contain all the discharge, as shown in figure 18. No HEC-2 runs were made for Drainage Basin I due to lack of runoff data at gauging station 3.

Another HEC-2 simulation considered the entire site area as one channel. As shown in figure 19, water flow became focused on the south part of the site, leaving the north part outside of the 100-yr floodplain. However, this result is based on the assumption that the drainage divides between subbasins I, II, and III do not prevent the surface runoff from coalescing into a single channel. It is important to recall that HEC-2 was designed for modeling flow in well-defined channels and does not perform well in modeling overland flow.

Runoff analyses with HEC-2 were made on a larger scale for the interarroyo area between the lower fork of Alamo Arroyo and the upper fork of Camp Rice Arroyo.

The tributary option in HEC-2 was used for the Alamo Arroyo, whereas only one channel was considered for the Camp Rice Arroyo, which has a well-defined channel (fig. 20). The number of cross sections was dictated by the ability of the HEC-2 model to solve the internal continuity and transport equations, given the range of topographic relief. The total potential and kinetic energy of flow in converging tributaries was also matched by adjusting cross-section orientations. Results from HEC-2 runs for the 100-yr flood are shown in figure 21. Different discharge for each cross section was used in the HEC-2 runs, reflecting the cumulative increase in upstream drainage area as one moves downstream (table 11). Figures 22 and 23 represent the channel configurations and the results for the probable maximum flood (PMF). The different tributary-channel configurations of the 100-yr runoff and the PMF in the Alamo Arroyo watershed (figs. 20 and 22) were based on the capacity of channels within each subbasin to contain the flow within the boundaries of that subbasin. Different channel configurations were required for 100-yr and PMF floods to maintain spatial continuity of flow in subbasins I and II. This was needed to force the HEC-2 simulations to distribute flow adequately on the relatively flat upland surface. If the 100-yr flood were modeled using the channel confuguration used to simulate the PMF flood (fig. 22), tributaries converging from subbasins I and II, then flow would be concentrated in the lower main channel downstream of section 6 (fig. 22), and flow in the upper channel at sections 13 to 16 (fig. 20) would be dried up. If the PMF flood were modeled using the channel configuration used to simulate the 100-yr flood (fig. 20), channels converging at the downstream edge of the site, then flow in the upper channel downstream of section 17 (fig. 20) would spill across the drainage divide from subbasin I to subbasin II. The flood widths plotted in figures 20 and 22 are the total widths of the wetted areas in the channels. The 0.5-ft flood heights are of course contained within these wetted areas.

CONCLUSIONS

Calculations following the alluvial fan evaluation indicate that the proposed site is in the area of the 100-yr floodplain (fig. 17). The procedure developed by Dawdy (FEMA, 1985) assumes the presence of active channels on an alluvial fan. The study area, however, is interpreted to be an alluvial plain or alluvial slope and not a fan (T. Gustavson, personal communication, 1989). Moreover, the results are sensitive to the arbitrary designation of the fan apex and to the expansion angle, although they ignore storage in existing channels and the presence of drainage divides that would act as barriers to flow. The alluvial-fan method was applied, nonetheless, to consider the range of possible flood potentials completely. Application of the Dawdy method results in a fan width of 118,600 ft, which would place the floodplain boundary farther downstream than any possibly definable alluvial plain (fig. 17), representing an absurdly extensive alluvial fan on the interarroyo plain. There is no sediment record of such an extensive flood with a return frequency of 0.01.

Surface-water runoff simulated with HEC-1 and HEC-2 tends to be concentrated in the relatively better defined channel in the south part of the study area in Drainage Basin III (fig. 2). The absence of well-incised channels in the central and north part result in shallow sheet-flow-type runoff in those areas. Due to the flat topography at the site, the selection of drainage boundaries between subbasins strongly influences the flood profiles in the channels (fig. 18). Removing the drainage boundary between the subbasins results in the whole runoff concentrating in the lower channel C in the south part of the study area (fig. 19).

The HEC-1 and HEC-2 flooding analyses for various basin and channel configurations indicate that most of the central study area contains large dry islands that are not inundated by 100-yr floods. The calculated runoff is contained in the

existing channels. There probably is some shallow-depth sheet flow over much of the rest of the area. The surface runoff resulting from a probable maximum flood increases the width of flood in the channels but still leaves uninundated islands in the central study area.

The best representation of the floodplain and channel configuration has the Camp Rice Arroyo watershed draining into a single channel and the Alamo Arroyo watershed draining into tributary channels. This model minimizes the sensitivity of flood profiles to numerous small drainage-basin boundaries. The runoff contribution of all the downstream sections is better incorporated under this scheme.

If a broad interpretation of the regulatory requirements is made and the separate dry islands are ignored, then most of the study area could be considered to be within a 100-yr floodplain. On the other hand, large sections of the interarroyo area between the lower fork of the Alamo Arroyo and the upper fork of the Camp Rice Arroyo would not be inundated, placing these sections outside of the 100-yr floodplain.

ACKNOWLEDGMENTS

This research was funded by the Texas Low-Level Radioactive Waste Disposal Authority. The conclusions of the authors are not necessarily approved or endorsed by the Authority.

The text was reviewed by A. R. Dutton and T. F. Hentz. Word processing was by Melissa Snell. Figures were drafted by Richard L. Dillon, as well as by Lisa L. Swan under Mr. Dillon's supervision.

REFERENCES

Baumgardner, R. W., 1989, Morphology of major arroyos in the vicinity of LLRW study area, Hudspeth County, Texas: The University of Texas at Austin, Bureau of Economic Geology, contract report prepared for Texas Low-Level Radioactive Waste Disposal Authority, under interagency contract number IAC(88-89)-0932, 17 p.

Chow, V. T., Maidment, D. R., and Mays, L. W., 1988, Applied hydrology: New York, McGraw-Hill, 572 p.

Espey, Huston, and Associates, Inc., 1981, Report on hydrologic investigations flood insurance study, Northwest El Paso, Texas, Phase I: Albuquerque, New Mexico, 26 p.

Federal Emergency Management Agency (FEMA), 1985, Federal insurance administration, guidelines and specifications for study contractors: FEMA 37, September 1985, p. 10-13.

Frederick, R. H., Myers, V. A., and Auciello, E. P., 1977, Five- to 60-minute precipitation frequency for the eastern and central United States: Soil Conservation Service, U. S. Department of Agriculture, NOAA Technical Memorandum NWS Hydro-35, Silver Spring, Maryland, p. 23-26.

Miller, J. F., Hansen, E. M., and Fenn, D. D., 1984, Probable maximum precipitation estimates - United States, between the Continental Divide and the 103rd meridian: U. S. Department of Interior Bureau of Reclamation, Hydrometeorological Report No. 55, Silver Spring, Maryland, p. 46-54.

Riggs, H. C., 1968, Techniques of water-resources investigations - frequency curves: U. S. Geological Survey, U. S. printing office, Arlington, Virginia, Book 4, Chapter A2, p. 4-5.

Soil Conservation Service, 1975, Urban hydrology for small watersheds: Washington, D. C., Technical Release No. 55, 82 p.

Texas Department of Water Resources, 1979a, Phase I inspection report, National Dam Safety Program, Alamo Arroyo WS Site No. 1, Hudspeth County, Texas: Austin, Texas Department of Water Resources, 48 p.

_____ 1979b, Phase I inspection report, National Dam Safety Program, Alamo Arroyo WS Site No. 3, Hudspeth County, Texas: Austin, Texas Department of Water Resources, 54 p.

_____ 1979c, Phase I inspection report, National Dam Safety Program, Camp Rice Arroyo WS Site No. 1, Hudspeth County, Texas: Austin, Texas Department of Water Resources, 68 p.

U. S. Army Corps of Engineers, 1981, HEC-1 flood hydrograph package: Davis, California, Hydrologic Engineering Center, 190 p.

U. S. Army Corps of Engineers, 1982, HEC-2 water surface profiles: Davis, California, Hydrologic Engineering Center, 40 p.

U. S. Department of the Interior, 1982, Guidelines for determining flood flow frequency: Washington, D. C., Interagency Advisory Committee on Water Data, Office of Water Data Coordination, Hydrology Subcommittee, Bulletin No. 17B, 35 p.

Table 1. Summary of surface-water runoff in channels at gauging stations and stillwell.

Date	Gauging Station 1	Gauging Station 2	Gauging Station 3	Stillwell 1
6/27-6/28	evaporation	not available	not available	not available
6/28-7/1	evap	n.a.	n.a.	n.a.
7/1-7/5	evap	n.a.	n.a.	32 in. @1510 hrs, 7/1
7/5-7/8	evap	n.a.	n.a.	evap
7/8-7/11	18 in. @0620 hrs, 7/10	plugged, not screened	n.a.	26.5 in. @0600 hrs, 7/10
7/11-7/14	evap	not screened	n.a.	evap
7/14-7/17	n.a.	not screened	n.a.	n.a.
7/17-7/20	evap	not screened	n.a.	n.a.
7/20-7/22	evap	evap	n.a.	evap
7/22-7/25	evap	evap	n.a.	evap
7/25-7/28	evap	~14 in. @1415 hrs, 7/27	n.a.	evap
7/28-7/31	~12 in. @1345 hrs, 7/29	~17 in. @1340 hrs, 7/29	n.a.	15.6 in. @1335 hrs, 7/29
7/31-8/3	evap	~6 in. @1920 hrs, 8/2	n.a.	evap
8/3-8/6	evap	~3.5 in. @1220 hrs, 8/5	n.a.	evap
8/6-8/9	~3 in. @1920 hrs, 8/7	~3.3 in. @1940 hrs, 8/7	n.a.	4.2 in. @1905 hrs, 8/7
8/9-8/12	evap	~7 in. @1240 hrs, 8/9	n.a.	0.85 in. @1335 hrs, 8/9
8/12-8/15	evap	evap	n.a.	evap
8/15-8/18	~1.5 in. @2200 hrs, 8/15	evap	n.a.	3.3 in. @2145 hrs, 8/15
8/18-8/21	evap	evap	n.a.	evap
8/21-8/24	evap	~14 in. @1430 hrs, 8/21	n.a.	evap
8/24-8/27	evap	~7 in. @1825 hrs, 8/26	n.a.	evap
8/27-8/30	evap	~2.5 in. @0605 hrs, 8/30	n.a.	3 in. @0115 hrs, 8/28
8/30-9/2	evap	evap	n.a.	evap
9/2-9/5	~5 in. @1305 hrs, 9/2	~9.1 in. @1315 hrs, 9/2	n.a.	evap
9/5-9/8	evap	evap	n.a.	evap
9/8-9/11	evap	evap	n.a.	evap
9/11-9/15	evap	evap	n.a.	evap
9/15-9/18	evap	evap	evap	evap
9/18-9/20	evap	evap	evap	evap
9/20-9/23	evap	~1.1 in. @2040 hrs, 9/21	~1.9 in. @1750 hrs, 9/20 ~2.2 in. @2020 hrs, 9/21	~1.3 in. @1910 hrs, 9/20 ~0.8 in. @2140 hrs, 9/21
9/23-9/26	evap	evap	evap	evap
9/26-9/29	evap	evap	evap	evap
9/29-10/2	evap	evap	evap	evap
10/2-10/5	evap	evap	evap	evap
10/5-10/8	evap	evap	evap	evap
10/8-10/11	evap	~0.7 in. @1250 hrs, 10/10	~1.7 in. @1240 hrs, 10/10	~0.4 in. @1730 hrs, 10/10
10/11-10/14	evap	evap	evap	evap
10/14-10/17	evap	evap	evap	evap
10/17-10/20	evap	evap	evap	evap
10/20-10/23	evap	evap	evap	evap
10/23-10/26	evap	evap	evap	evap
10/26-10/29	evap	evap	evap	evap
10/29-11/1	evap	evap	evap	evap
11/1-11/4	evap	evap	evap	evap
11/4-11/7	evap	evap	evap	evap
11/7-11/10	evap	evap	evap	evap
11/10-11/13	evap	evap	evap	evap
11/13-11/16	evap	evap	evap	evap
11/16-11/19	evap	evap	evap	evap
11/19-11/22	evap	evap	evap	evap
11/22-11/25	evap	evap	evap	evap
11/25-11/28	evap	evap	evap	evap
11/28-12/1	evap	evap	evap	evap
12/1-12/4	evap	evap	evap	evap

Table 1 (Continued)

Date	Gauging Station 1	Gauging Station 2	Gauging Station 3	Stillwell 1
12/4-12/7	evap	evap	evap	evap
12/7-12/10	evap	evap	evap	evap
12/10-12/13	evap	evap	evap	evap
12/13-12/16	evap	evap	evap	evap
12/16-12/19	evap	evap	evap	evap
12/19-12/22	evap	evap	evap	evap
12/22-12/25	evap	evap	evap	evap
12/25-12/28	evap	evap	evap	evap
12/28-12/31	evap	evap	evap	evap
12/31-1/3/89	evap	evap	evap	evap
1/3-1/6	evap	evap	evap	evap
1/6-1/9	evap	evap	evap	evap
1/9-1/12	evap	evap	evap	evap
1/12-1/15	evap	evap	evap	evap
1/15-1/18	evap	evap	evap	evap
1/18-1/21	evap	evap	evap	evap
1/21-1/24	evap	evap	evap	evap
1/24-1/27	evap	evap	evap	evap
1/27-1/30	evap	evap	evap	evap
1/30-2/2	evap	evap	evap	evap
2/2-2/5	evap	evap	evap	evap
2/5-2/8	evap	evap	evap	evap
2/8-2/11	evap	evap	evap	evap
2/11-2/14	evap	evap	evap	evap
2/14-2/17	evap	evap	evap	~0.4 in. @1920 hrs, 12/16
2/17-2/20	evap	evap	evap	evap
2/20-2/23	evap	evap	evap	evap
2/23-2/26	evap	evap	evap	evap
2/26-3/1	evap	evap	evap	evap
3/1-3/4	evap	evap	evap	evap
3/4-3/7	evap	evap	evap	evap
3/7-3/10	evap	evap	evap	evap
3/10-3/13	evap	evap	evap	evap
3/13-3/16	evap	evap	evap	evap
3/16-3/19	evap	evap	evap	evap
3/19-3/22	evap	evap	evap	evap
3/22-3/25	evap	evap	evap	evap
3/25-3/28	evap	evap	evap	evap
3/28-3/31	evap	evap	evap	evap
3/31-4/3	evap	evap	evap	evap
4/3-4/6	evap	evap	evap	evap
4/6-4/9	evap	evap	evap	evap
4/9-4/12	evap	evap	evap	evap
4/12-4/15	evap	evap	evap	evap
4/15-4/18	evap	evap	evap	evap
4/18-4/21	evap	evap	evap	evap
4/21-4/24	evap	evap	evap	evap
4/24-4/27	evap	evap	evap	evap
4/27-4/30	evap	evap	evap	evap
4/30-5/3	evap	evap	evap	evap
5/3-5/6	evap	evap	evap	evap
5/6-5/9	evap	evap	evap	evap
5/9-5/12	evap	~2.0 in. @2050 hrs, 5/9	evap	evap
5/12-5/15	evap	evap	evap	evap
5/15-5/18	evap	evap	evap	evap

Table 1 (Continued)

Date	Gauging Station 1	Gauging Station 2	Gauging Station 3	Stillwell 1
5/18-5/21	evap	evap	evap	evap
5/21-5/24	evap	evap	evap	evap
5/24-5/27	evap	evap	evap	evap
5/27-5/30	evap	~3.7 in. @2100 hrs, 5/27	~2.5 in. @2120 hrs, 5/27	evap
5/30-6/2	evap	evap	evap	evap
6/2-6/5	evap	evap	evap	evap
6/5-6/8	evap	evap	evap	evap
6/8-6/11	evap	evap	evap	evap
6/11-6/14	evap	evap	evap	~0.72 in. @1925 hrs, 6/13
6/14-6/17	evap	evap	evap	evap
6/17-6/20	evap	evap	evap	evap
6/20-6/23	~8.04 in. @1915 hrs, 6/20	evap	~2.7 in. @1920 hrs, 6/20	evap
6/23-6/26	evap	evap	evap	evap
6/26-6/29	evap	evap	evap	evap
6/29-7/2	evap	evap	evap	evap
7/2-7/5	evap	evap	evap	evap
7/5-7/8	evap	evap	evap	evap
7/8-7/11	evap	evap	evap	evap
7/11-7/14	evap	evap	evap	evap
7/14-7/17	evap	evap	evap	evap
7/17-7/20	evap	evap	evap	evap
7/20-7/23	evap	evap	evap	evap
7/23-7/26	evap	evap	evap	evap
7/26-7/29	evap	evap	evap	evap
7/29-8/1	~0.84 in. @0315 hrs, 7/30	~2.3 in. @0300 hrs, 7/30	~2.4 in. @0300 hrs, 7/30	~0.48 in. @0335 hrs, 7/30

Table 2. Rainfall data (mm) for 07-29-88 event, recorded at the 5 rain gauges.

TIME(from)	TIME(to)	Rain gauge 1	Rain gauge 2	Rain gauge 3	Rain gauge 4	Rain gauge 5
13:05	13:10		0.60		n.a.	0.25
13:10	13:15		1.00	0.60	n.a.	0.25
13:15	13:20		2.00	0.60	n.a.	0.13
13:20	13:25	3.40	3.00	0.70	n.a.	0.13
13:25	13:30	3.40	3.00	0.70	n.a.	0.38
13:30	13:35	2.00	2.00	0.60	n.a.	0.38
13:35	13:40	0.50	2.00		n.a.	1.27
13:40	13:45	0.50	1.00		n.a.	1.27
13:45	13:50	1.00	1.00		n.a.	3.05
13:50	13:55	1.00	0.60	4.00	n.a.	3.05
13:55	14:00	0.40	0.60	4.00	n.a.	1.78
14:00	14:05	0.40		10.00	n.a.	1.78
14:05	14:10	0.60		10.00	n.a.	2.03
14:10	14:15	0.60	0.40	3.00	n.a.	2.03
14:15	14:20	1.10	0.40	3.00	n.a.	1.27
14:20	14:25	1.10	1.20	0.30	n.a.	1.27
14:25	14:30	0.30	1.20	0.30	n.a.	
14:30	14:35	0.30	0.30		n.a.	
14:35	14:40	2.00	0.30		n.a.	
	total =	16.80	20.60	37.80	- -	20.32
average (of 4 gauges) =		23.88				

Table 3. Rainfall data (mm) for 08-02-88 event, recorded at the 5 rain gauges.

TIME(from)	TIME(to)	Rain gauge 1	Rain gauge 2	Rain gauge 3	Rain gauge 4	Rain gauge 5
18:50	18:55	1.40			n.a.	
18:55	19:00	1.40	1.00		n.a.	
19:00	19:05	1.00	1.00		n.a.	
19:05	19:10	1.00	1.00		n.a.	
19:10	19:15	0.20	0.30	1.70	n.a.	0.63
19:15	19:20		0.30	1.70	n.a.	0.64
19:20	19:25		0.10	1.40	n.a.	3.18
19:25	19:30		0.10	1.40	n.a.	3.18
19:30	19:35			0.30	n.a.	0.51
19:35	19:40			0.30	n.a.	0.51
19:40	19:45			0.10	n.a.	0.50
19:45	19:50			0.10	n.a.	0.13
19:50	19:55				n.a.	0.13
19:55	20:00				n.a.	0.12
20:00	20:05				n.a.	0.12
	total =	5.00	3.80	7.00	- -	9.65
average (of 4 gauges) =		6.36				

Table 4. Rainfall data (mm) for 08-09-88 event, recorded at the 5 rain gauges.

TIME(from)	TIME(to)	Rain gauge 1	Rain gauge 2	Rain gauge 3	Rain gauge 4	Rain gauge 5
12:30	12:35			0.60	n.a.	0.38
12:35	12:40			0.60	n.a.	0.38
12:40	12:45			0.50	n.a.	0.26
12:45	12:50			0.50	n.a.	0.25
12:50	12:55				n.a.	0.13
12:55	13:00				n.a.	0.12
13:00	13:05				n.a.	
13:05	13:10				n.a.	
13:10	13:15				n.a.	
13:15	13:20				n.a.	
13:20	13:25				n.a.	
13:25	13:30				n.a.	
13:30	13:35	0.70		2.80	n.a.	0.41
13:35	13:40	0.70	0.40	2.80	n.a.	0.42
13:40	13:45	0.60	0.70	0.60	n.a.	2.00
13:45	13:50		0.70	0.60	n.a.	2.00
13:50	13:55		0.10		n.a.	1.53
13:55	14:00		0.10		n.a.	1.52
14:00	14:05			0.10	n.a.	0.13
14:05	14:10	0.20		0.10	n.a.	0.13
14:10	14:15	0.20	0.10	0.20	n.a.	0.13
14:15	14:20		0.10	0.20	n.a.	0.13
14:20	14:25			0.10	n.a.	0.12
14:25	14:30			0.10	n.a.	0.12
	total =	2.40	2.20	9.80	- -	10.16
average (of 4 gauges) =		6.14				

Table 5. Rainfall data (mm) for 08-21-88 event, recorded at the 5 rain gauges.

TIME(from)	TIME(to)	Rain gauge 1	Rain gauge 2	Rain gauge 3	Rain gauge 4	Rain gauge 5
14:00	14:05			0.60		
14:05	14:10			4.00		
14:10	14:15			3.50		
14:15	14:20			3.50		
14:20	14:25			3.00		
14:25	14:30			2.00		
14:30	14:35			0.30		0.25
14:35	14:40			0.30	0.40	0.26
14:40	14:45	1.00		0.10	4.50	0.76
14:45	14:50	1.00	0.40	0.10	4.50	0.76
14:50	14:55	0.50	0.80	0.10	2.00	1.16
14:55	15:00	0.50	0.80	0.10	2.00	1.16
15:00	15:05	0.20	0.30		0.50	1.16
15:05	15:10	0.20	0.30		0.50	1.17
15:10	15:15		0.20		0.20	1.16
15:15	15:20		0.20		0.20	1.16
15:20	15:25		0.10		0.10	1.16
15:25	15:30		0.10		0.10	0.51
15:30	15:35					0.51
15:35	15:40					0.13
15:40	15:45					0.12
15:45	15:50					0.07
15:50	15:55					0.07
15:55	16:00					0.06
16:00	16:05					0.06
	total =	3.40	3.20	17.60	15.00	11.69

average (of 5 gauges) = 10.18

Table 6. Rainfall data (mm) for 09-02-88 event, recorded at the 5 rain gauges.

TIME(from)	TIME(to)	Rain gauge 1	Rain gauge 2	Rain gauge 3	Rain gauge 4	Rain gauge 5
12:55	13:00			0.80		
13:00	13:05			3.00		
13:05	13:10	3.30		3.00		
13:10	13:15	3.30		0.90		
13:15	13:20	3.50	2.40	0.90		
13:20	13:25	3.50	1.50	0.20		
13:25	13:30	0.70	1.50	0.20		
13:30	13:35	0.70	0.70			0.76
13:35	13:40	0.20	0.70			0.77
13:40	13:45					3.43
13:45	13:50					3.43
13:50	13:55					0.76
13:55	14:00					0.76
	total =	15.20	6.80	9.00	0.00	9.91

average (of 5 gauges) = 8.18

Table 7. Optimized LS card (SCS curve number) parameters for gauging station 2.

	Channel cross-sections							
	x-sec w/road		x-sec w/out road		x-sec 50 ft upstream		x-sec 63 ft upstream	
DATE	STRTL	CN	STRTL	CN	STRTL	CN	STRTL	CN
7/29/88	19.68	88.39	21.20	88.95	19.00	80.28	20.44	81.45
8/02/88	5.32	81.88	5.32	81.88	5.48	81.78	5.96	86.31
8/09/88	4.44	79.40	4.44	79.40	3.99	67.74	4.84	72.99
8/21/88	4.96	77.85	6.43	81.88	6.72	84.24	6.08	68.21
9/02/88	7.50	90.02	7.50	90.02	7.54	89.50	7.71	86.98

STRTL (mm) : initial abstraction before ponding
average value = 8.73
standard deviation = 5.79

CN : SCS curve number
average value = 81.96
standard deviation = 6.45

Table 8. Optimized LU card (uniform loss) parameters for gauging station 2.

	Channel cross-sections							
	x-sec w/road		x-sec w/out road		x-sec 50 ft upstream		x-sec 63 ft upstream	
DATE	STRTL	CN	STRTL	CN	STRTL	CN	STRTL	CN
7/29/88	22.72	3.85	23.27	1.61	22.87	4.10	23.27	1.74
8/02/88	6.56	0.66	6.56	0.66	6.60	0.66	6.71	0.67
8/09/88	5.91	0.84	5.91	0.84	5.90	0.85	6.37	0.64
8/21/88	8.46	2.98	9.54	1.32	9.51	1.39	9.76	1.13
9/02/88	8.07	0.54	8.07	0.54	8.08	0.54	8.09	0.54

STRTL (mm) : initial abstraction before ponding
average value = 10.61
standard deviation = 6.32

CNSTL (mm/hr) : constant loss rate
average value = 1.31
standard deviation = 1.06

Table 9. Percentage of rainfall lost to infiltration.

Date	Rainfall (mm)	Loss (mm)	Loss %	Cumulative Rainfall (mm) Since Previous Event
7/29/88	23.88	23.575	98.73	2.00
8/02/88	6.36	6.348	99.80	0.90
8/09/88	6.14	6.105	99.43	23.38
8/21/88	10.18	9.975	97.99	8.62
9/02/88	8.18	8.165	99.82	24.65
100-YR STORM	86.36	43.17	49.99	

Table 10. Five-minute interval distributions (inches) of 100-year and PMP precipitation.

TIME (HR:MIN)	100-YEAR	PMP	TIME (HR:MIN)	100-YEAR	PMP
0:05	0.00	0.01	3:05	0.05	3.19
0:10	0.00	0.02	3:10	0.09	1.18
0:15	0.00	0.02	3:15	0.09	0.94
0:20	0.00	0.03	3:20	0.06	0.89
0:25	0.00	0.03	3:25	0.11	0.71
0:30	0.00	0.04	3:30	0.12	0.71
0:35	0.00	0.05	3:35	0.36	0.27
0:40	0.00	0.05	3:40	0.62	0.26
0:45	0.00	0.05	3:45	0.61	0.25
0:50	0.00	0.05	3:50	0.24	0.22
0:55	0.00	0.05	3:55	0.23	0.19
1:00	0.00	0.05	4:00	0.14	0.15
1:05	0.00	0.07	4:05	0.04	0.14
1:10	0.00	0.08	4:10	0.04	0.14
1:15	0.00	0.08	4:15	0.04	0.13
1:20	0.00	0.08	4:20	0.03	0.13
1:25	0.00	0.08	4:25	0.04	0.13
1:30	0.00	0.10	4:30	0.04	0.13
1:35	0.00	0.12	4:35	0.03	0.10
1:40	0.00	0.13	4:40	0.04	0.10
1:45	0.00	0.13	4:45	0.04	0.08
1:50	0.00	0.13	4:50	0.03	0.08
1:55	0.00	0.14	4:55	0.04	0.08
2:00	0.00	0.14	5:00	0.04	0.07
2:05	0.01	0.15	5:05	0.00	0.06
2:10	0.02	0.18	5:10	0.00	0.05
2:15	0.02	0.21	5:15	0.00	0.05
2:20	0.02	0.24	5:20	0.00	0.05
2:25	0.02	0.26	5:25	0.00	0.05
2:30	0.02	0.27	5:30	0.00	0.04
2:35	0.02	0.59	5:35	0.00	0.04
2:40	0.02	0.71	5:40	0.00	0.03
2:45	0.02	0.89	5:45	0.00	0.03
2:50	0.02	0.89	5:50	0.00	0.02
2:55	0.02	1.12	5:55	0.00	0.02
3:00	0.02	1.54	6:00	0.00	0.01

Table 11. Discharges (cfs) used in HEC-2 for tributary-flow option.

100 Year Flood

x-section #	Alamo Arroyo	Camp Rice Arroyo
1	19290	17110
2	18870	16780
3	18560	16570
4	18070	16240
5	17490	15870
6	13760	15440
7	13440	15010
8	12490	14530
9	3050	14040
10	2470	
11	8900	
12	8130	
13	8140	
14	7990	
15	7620	
16	7160	
17	6600	
18	6070	
19	5030	
20	3790	

Probable Maximum Flood

x-section #	Alamo Arroyo	Camp Rice Arroyo
1	157710	142900
2	153650	139390
3	150590	137200
4	145910	133730
5	140280	129740
6	104810	125270
7	100840	120700
8	92490	115630
9	78590	110400
10	49080	
11	45030	
12	37020	
13	27480	

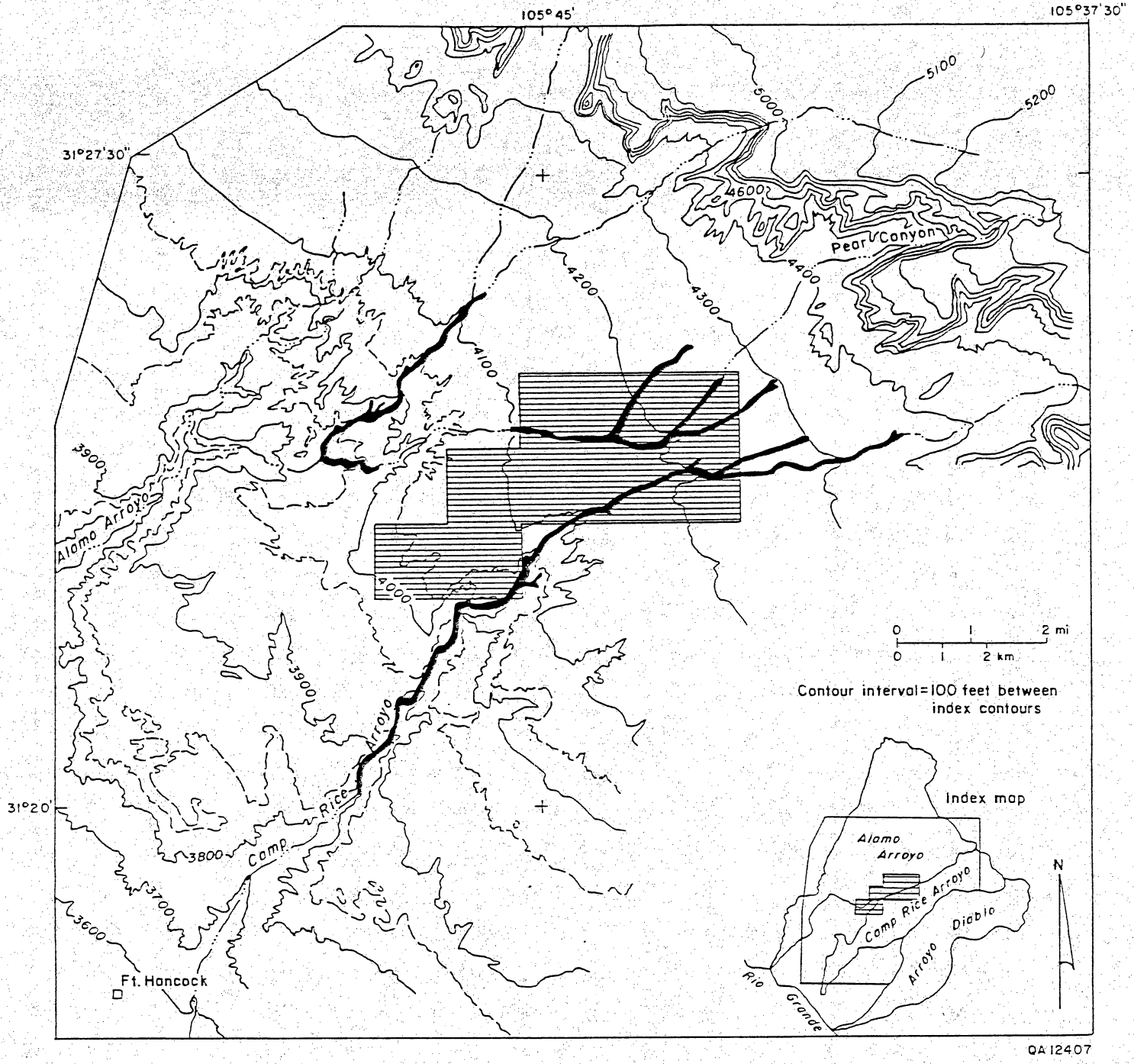

Figure 1. One-hundred-yr flood plain on proposed West Texas low-level radioactive waste isolation site (Federal Emergency Management Agency, 1985). Map does not include the boundary of 100-year flood plain in lower reaches of Camp Rice and Alamo Arroyo.

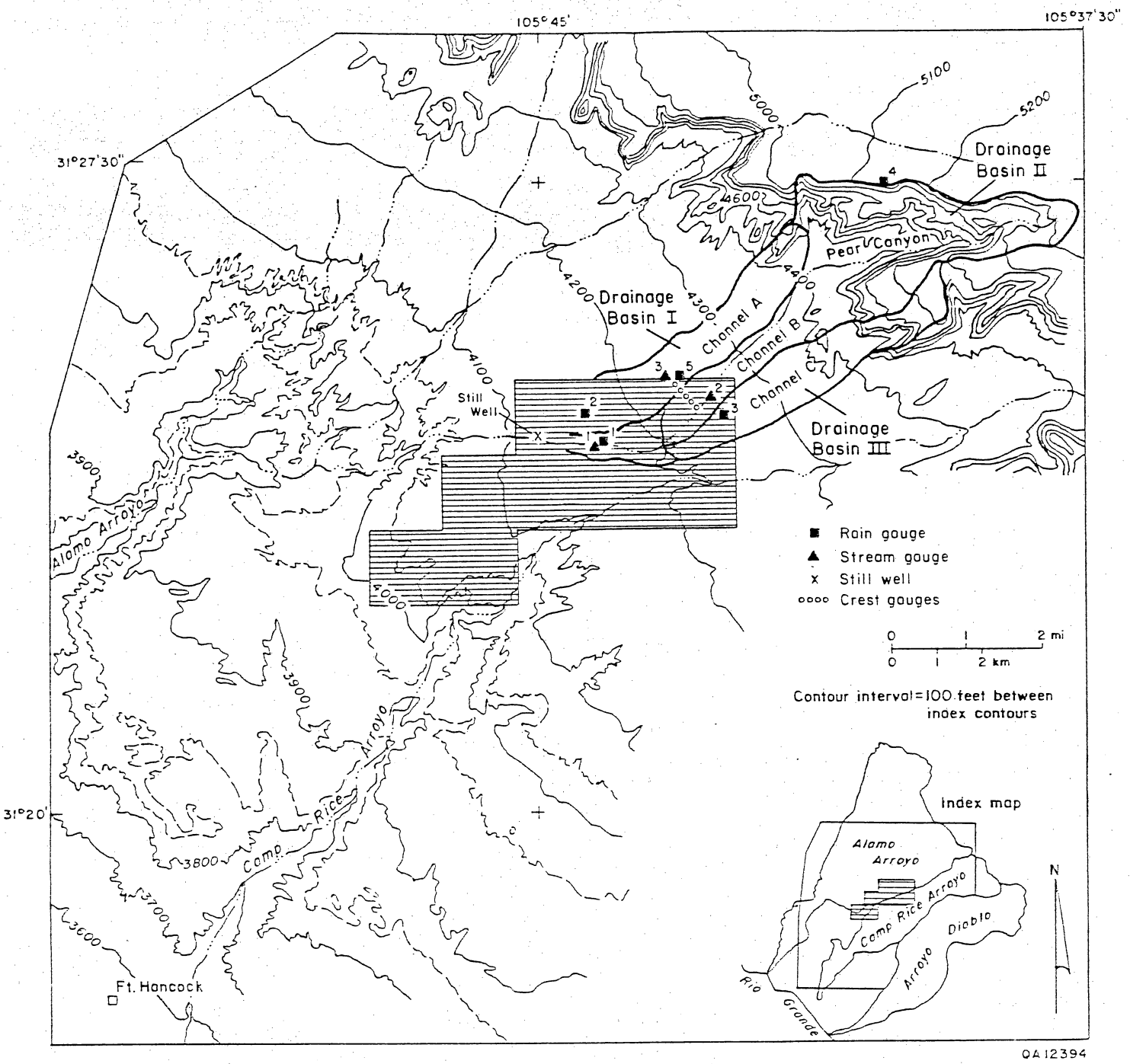

Figure 2. Surface-water hydrology study area and location of stream gauges and rain gauges. The drainage basins were delineated for determining flood profiles in the channels.

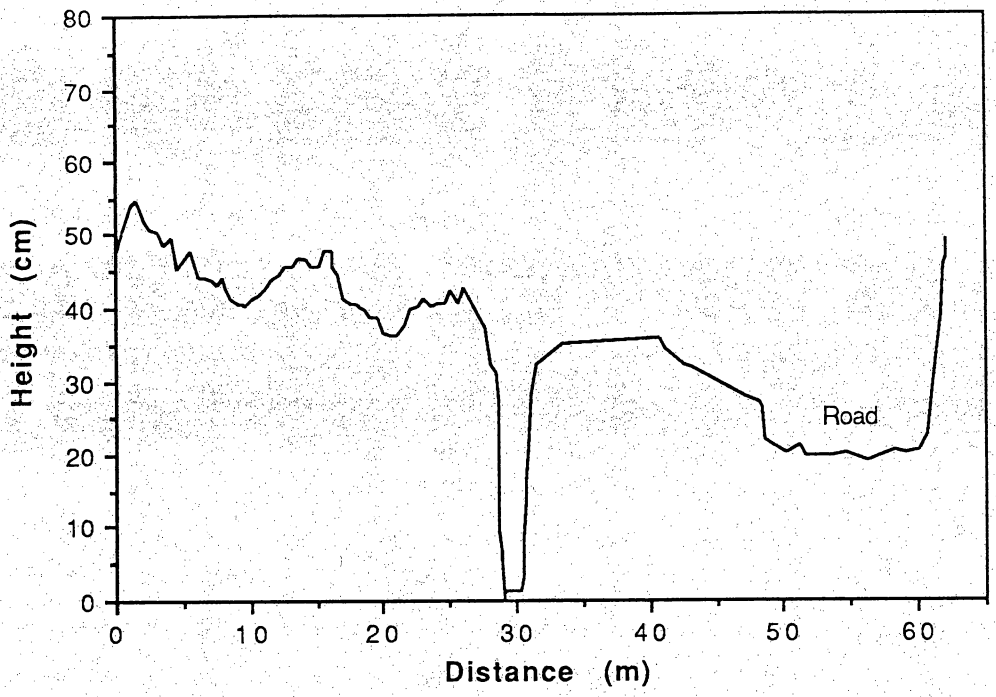

Figure 3. Cross-section profile of channel at gauging station 2. Part of the nearby unpaved road is included in the cross section.

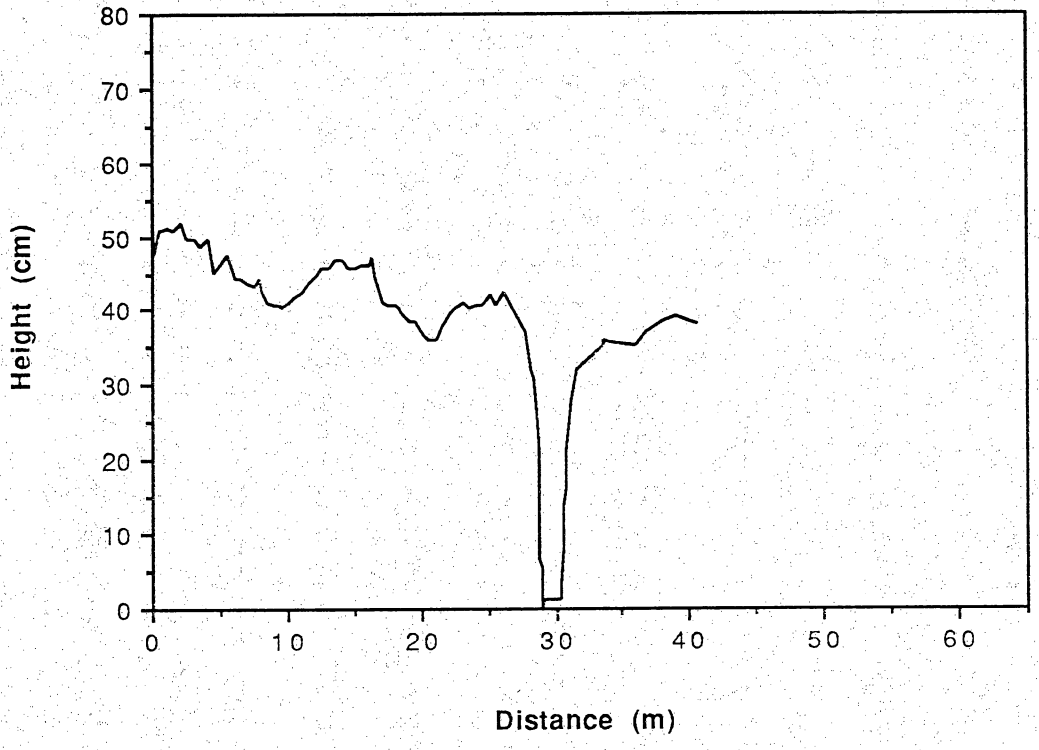

Figure 4. Cross-section profile of channel at gauging station 2. Nearby unpaved road section is excluded from the cross section.

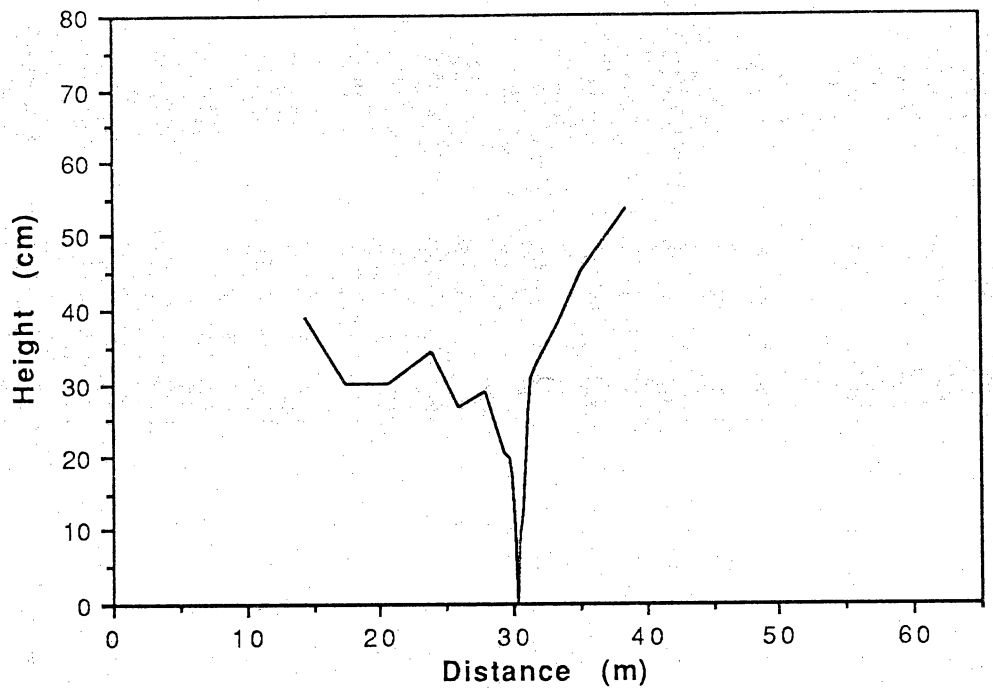

Figure 5. Channel cross-section profile 50 ft upstream of gauging station 2.

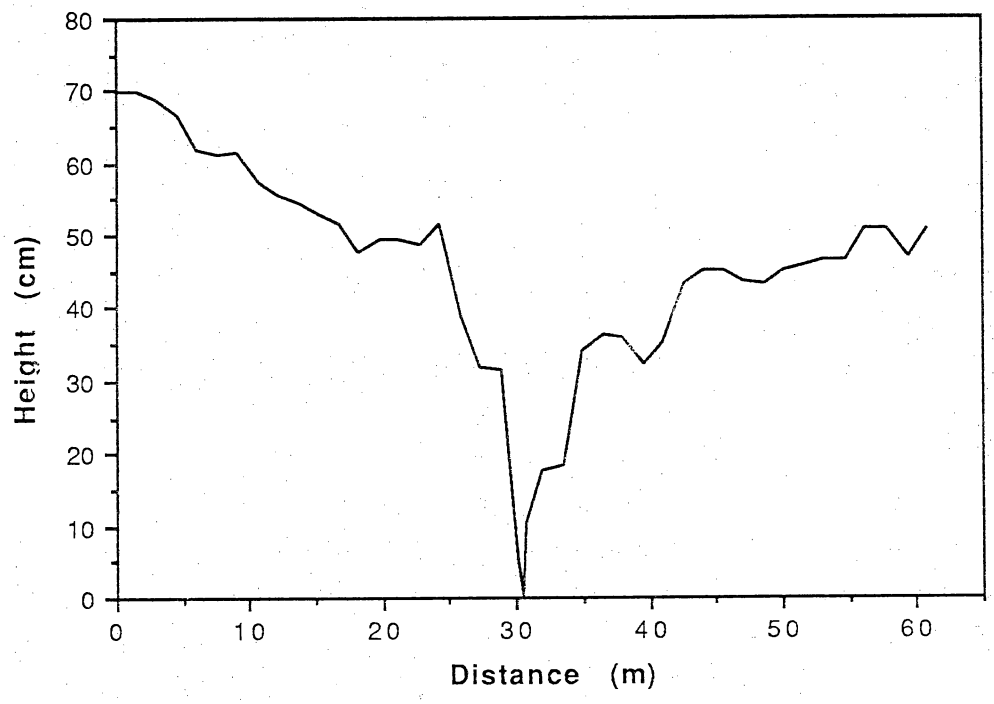

Figure 6. Channel cross-section profile 63 ft upstream of gauging station 2.

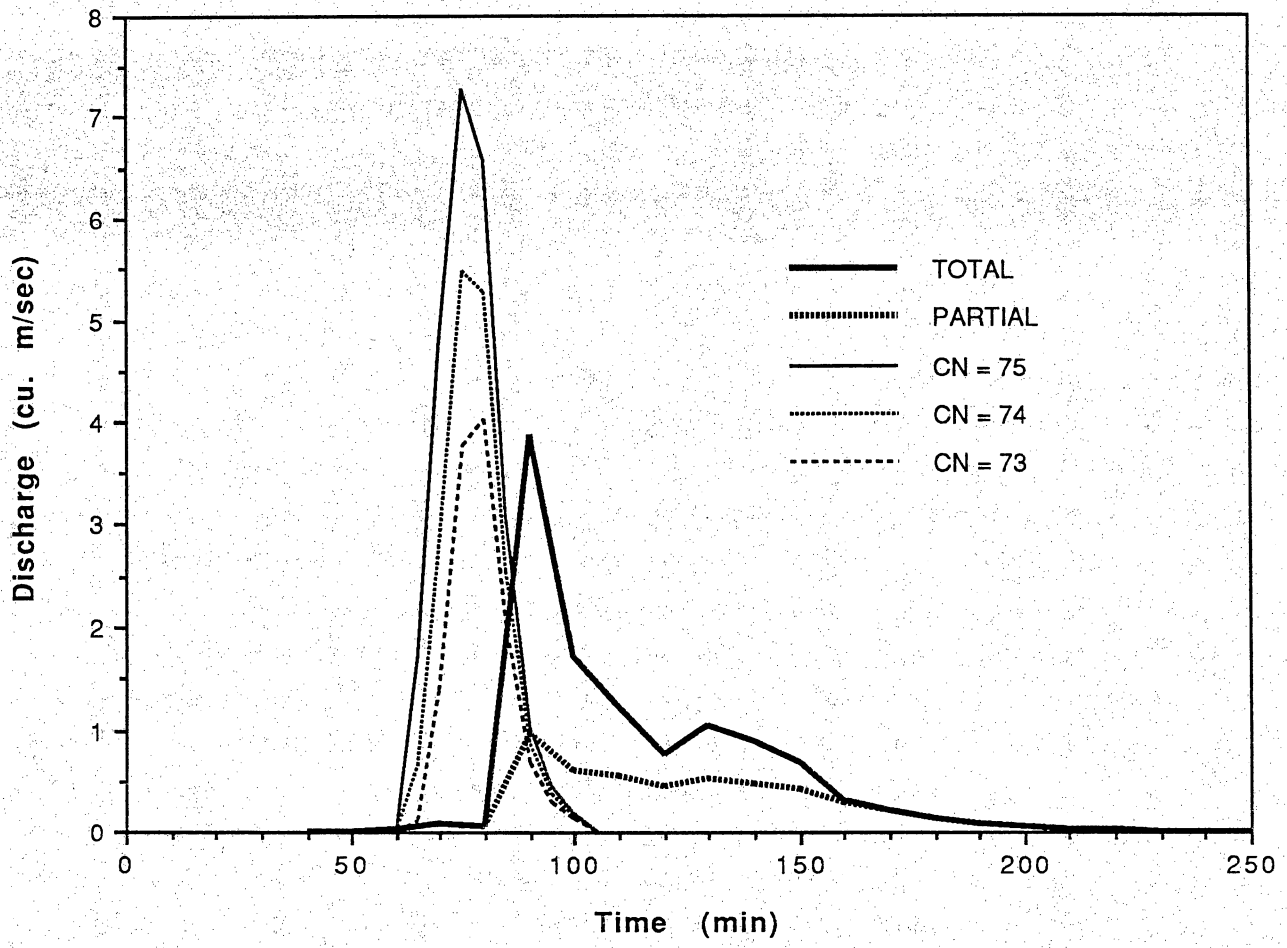

Figure 7. Hydrograph at gauging station 2 on 7-29-88 (whole basin model).

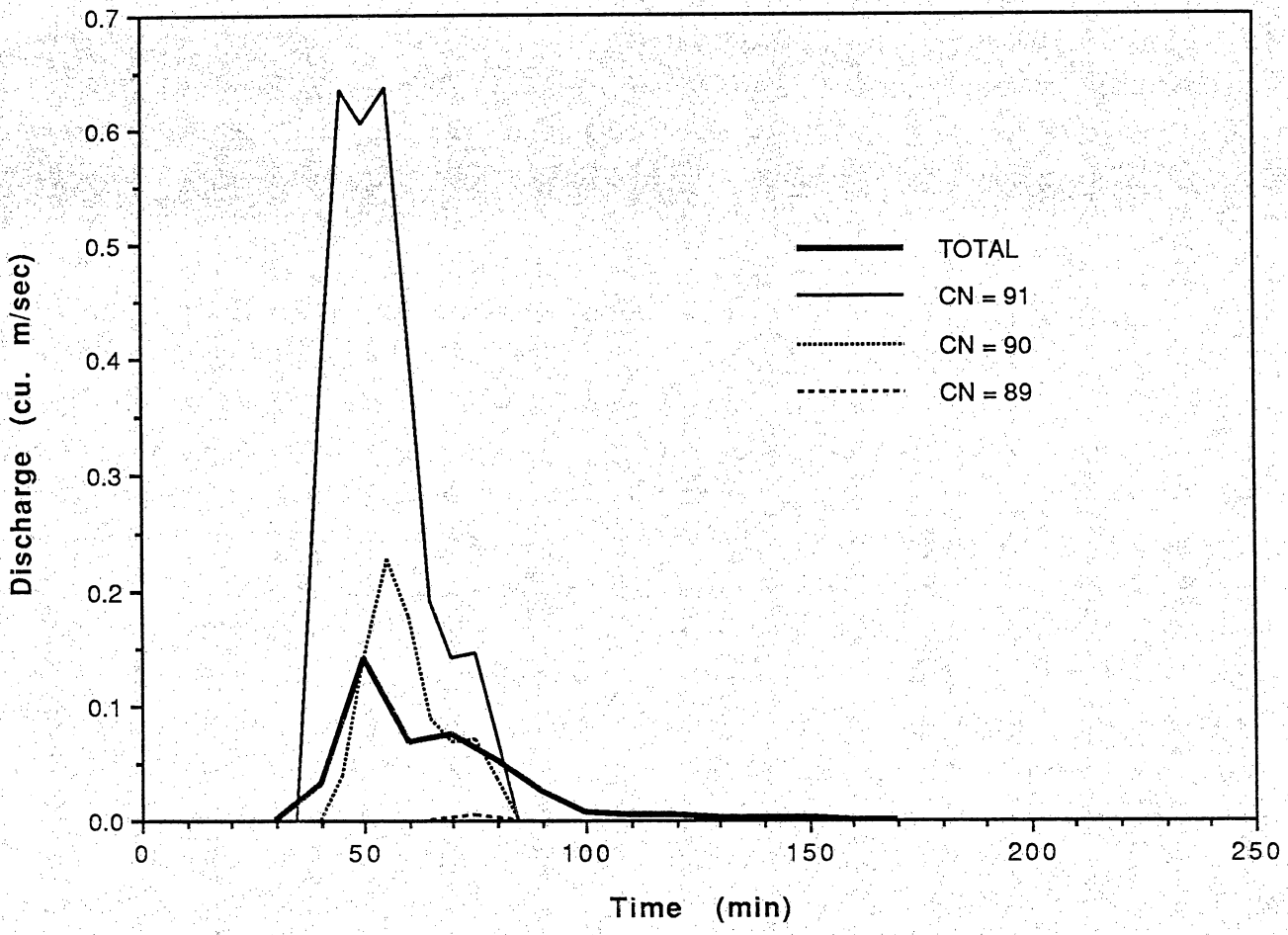

Figure 8. Hydrograph at gauging station 2 on 8-2-88 (whole basin model).

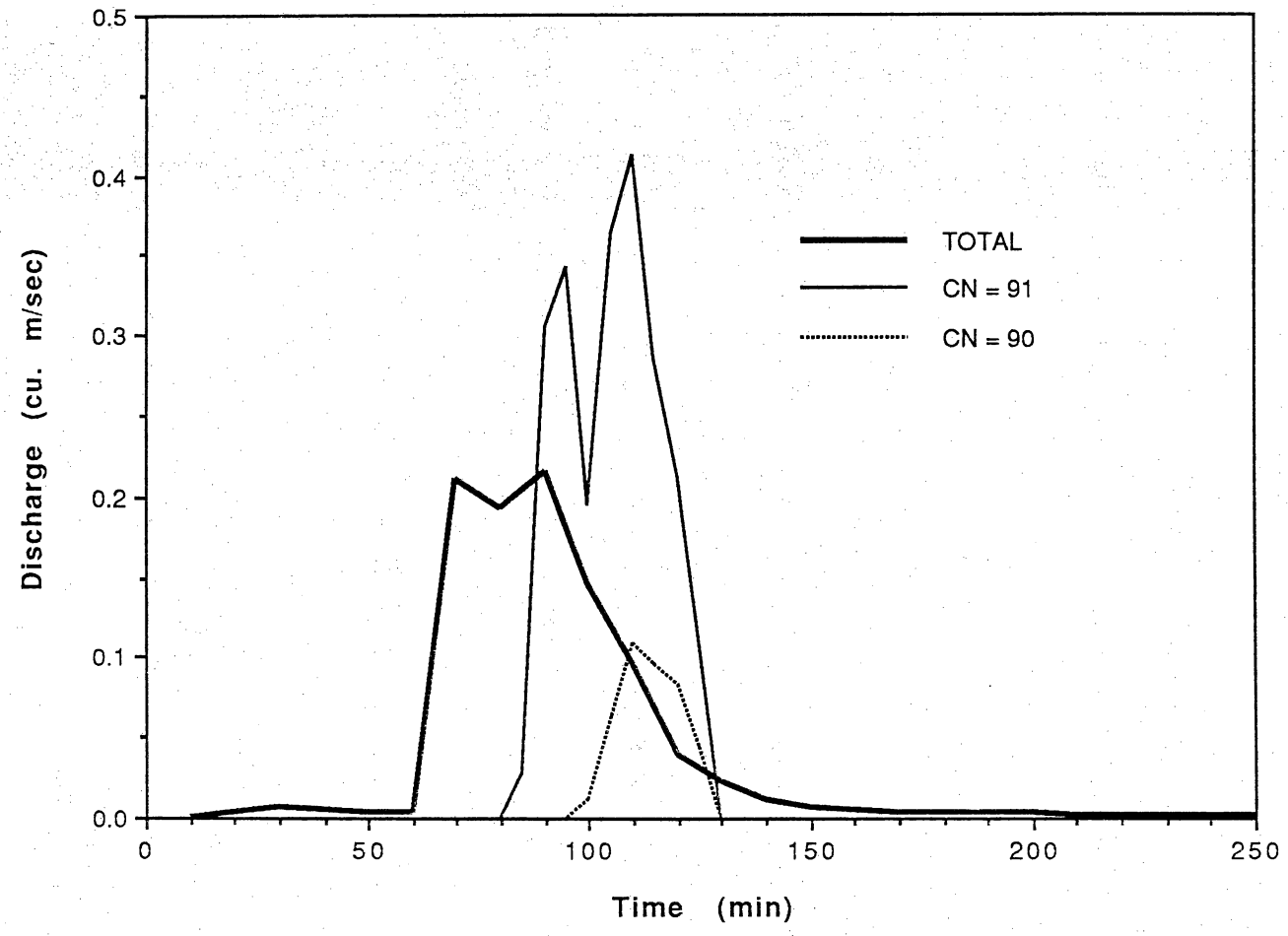

Figure 9. Hydrograph at gauging station 2 on 8-9-88 (whole basin mocel).

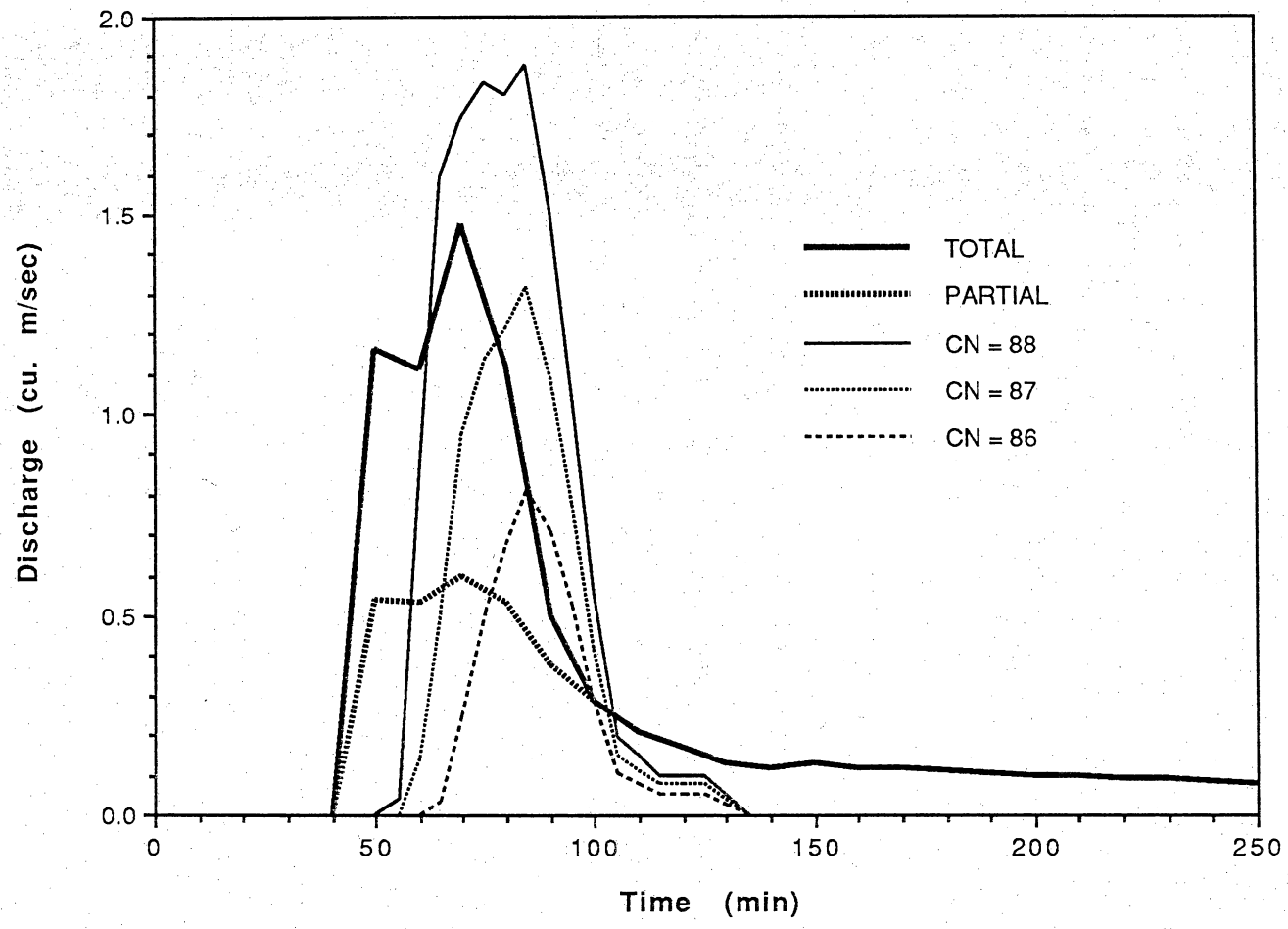

Figure 10. Hydrograph at gauging station 2 on 8-21-88 (whole basin model).

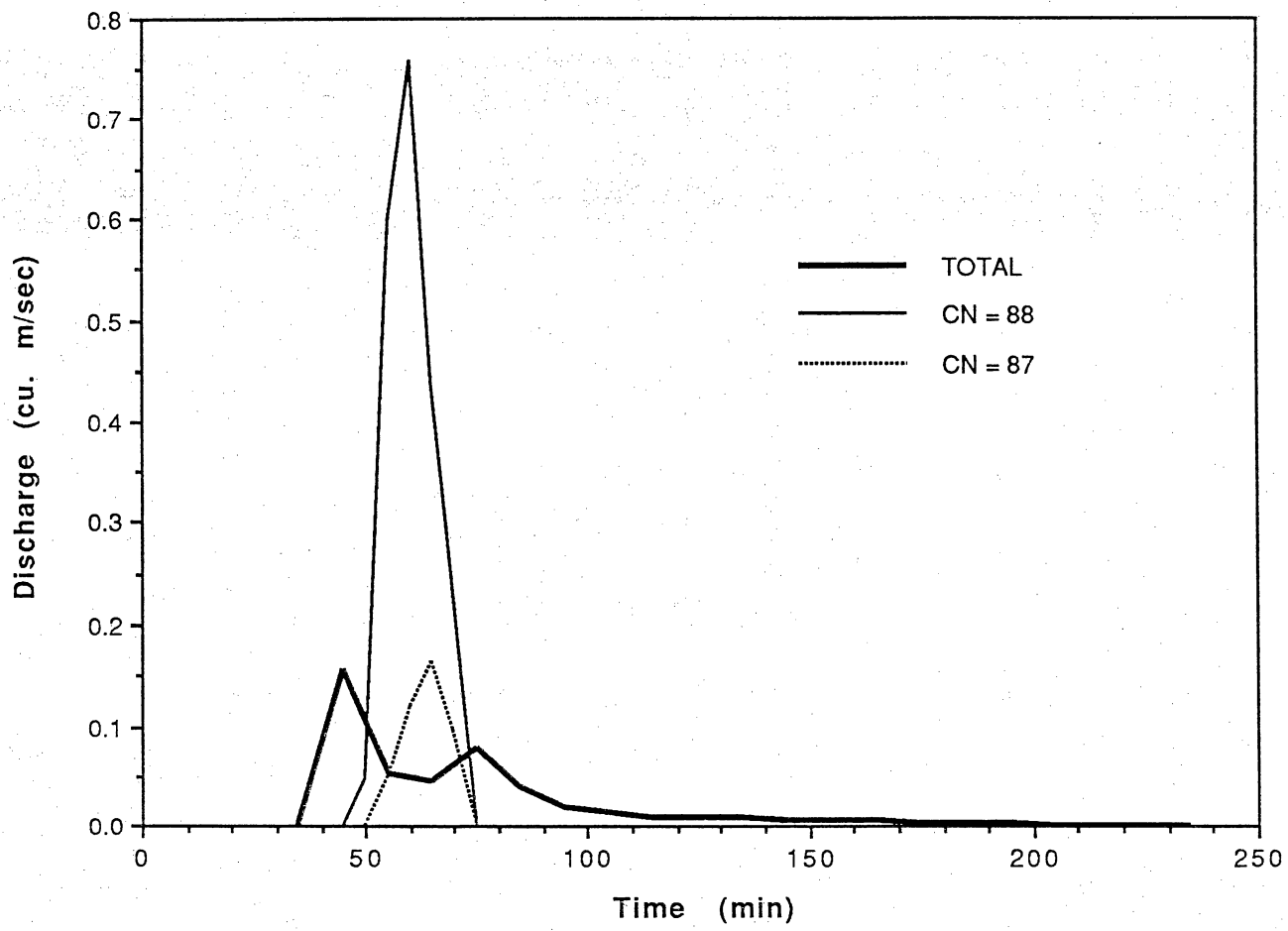

Figure 11. Hydrograph at gauging station 2 on 9-2-88 (whole basin model).

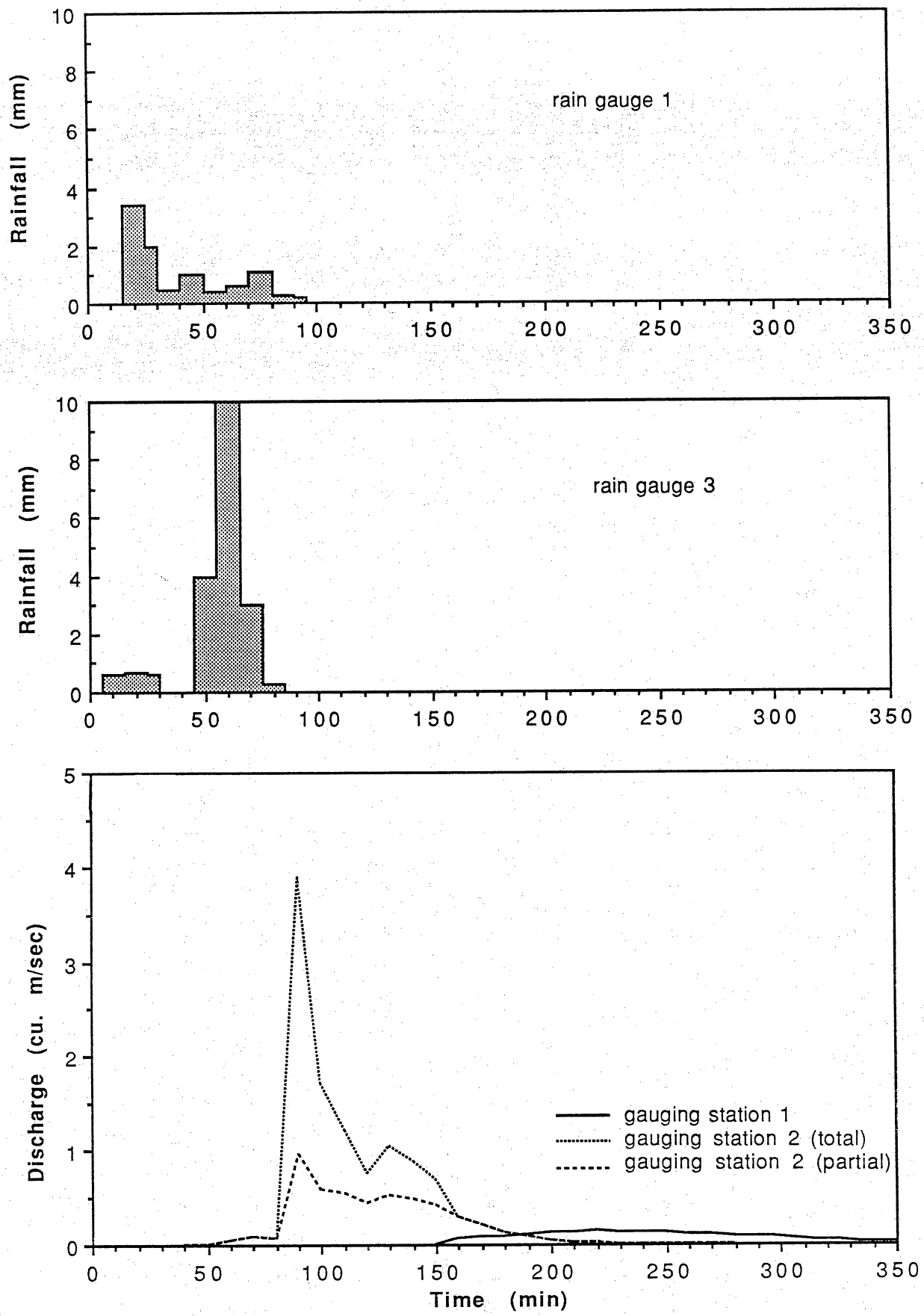

Figure 12. Comparison of observed hydrographs at gauging stations 1 and 2 and corresponding rainfall data.

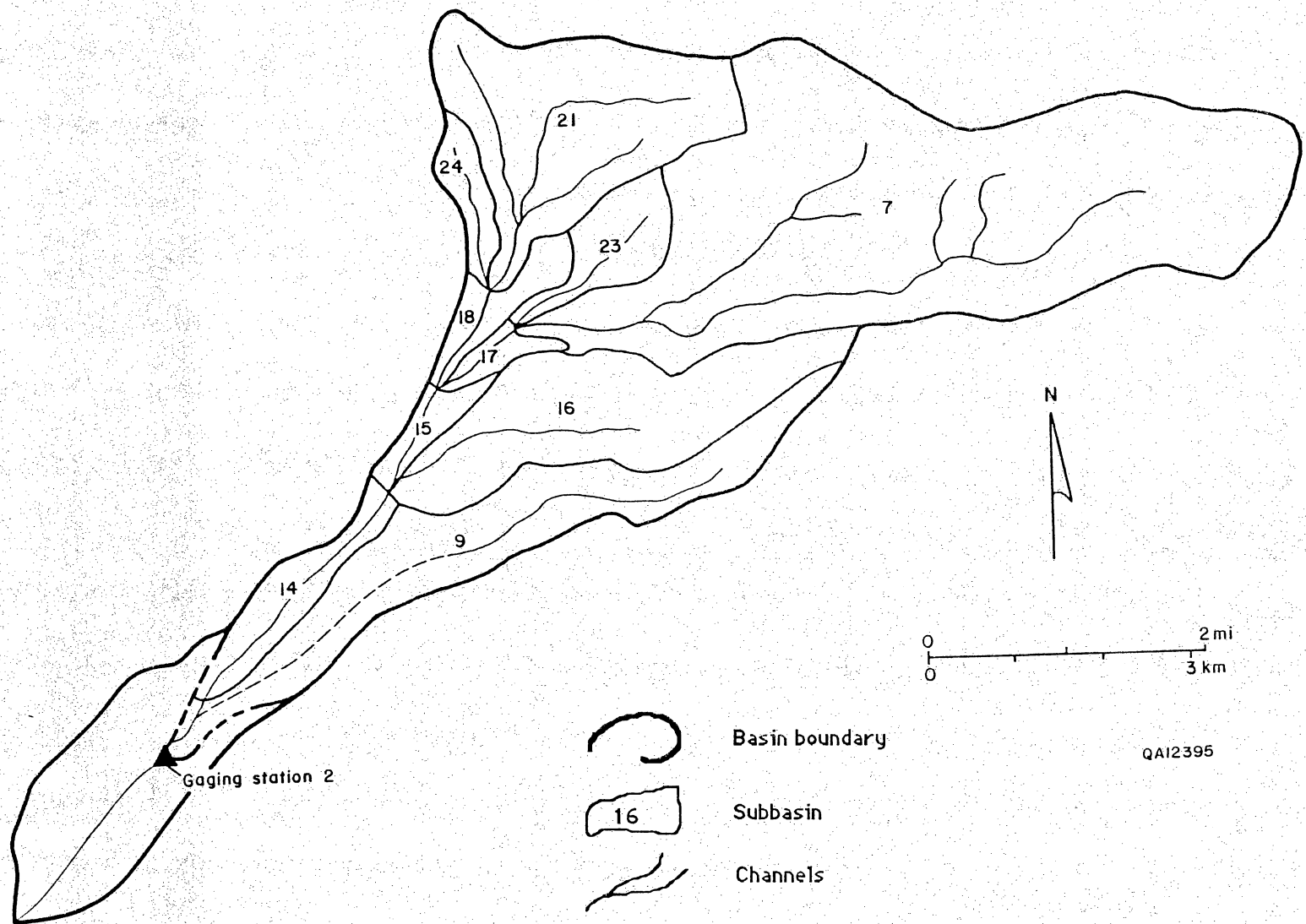

Figure 13. Subbasin configuration for HEC-1 kinematic routing model. Flow from drainage basin II measured at gauging station 2.

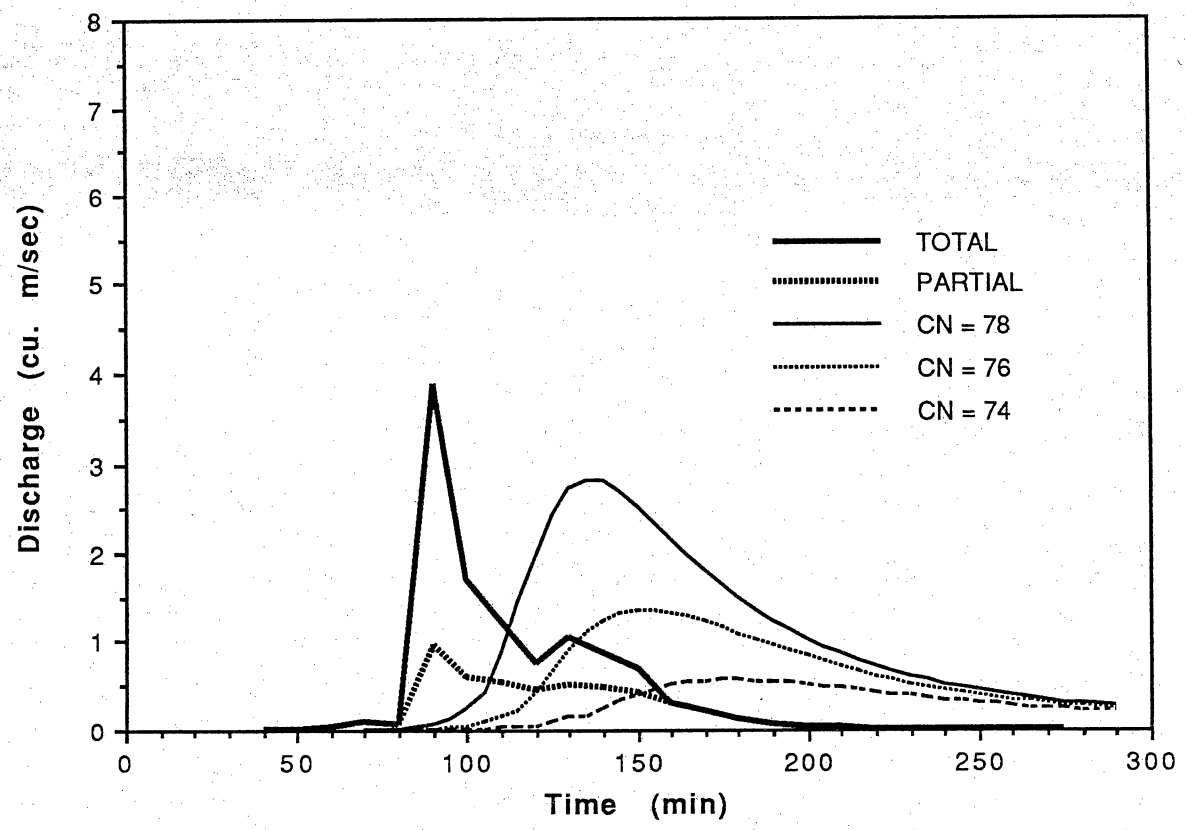

Figure 14. Hydrograph at gauging station 2 on 7-29-88 (kinematic routing model).

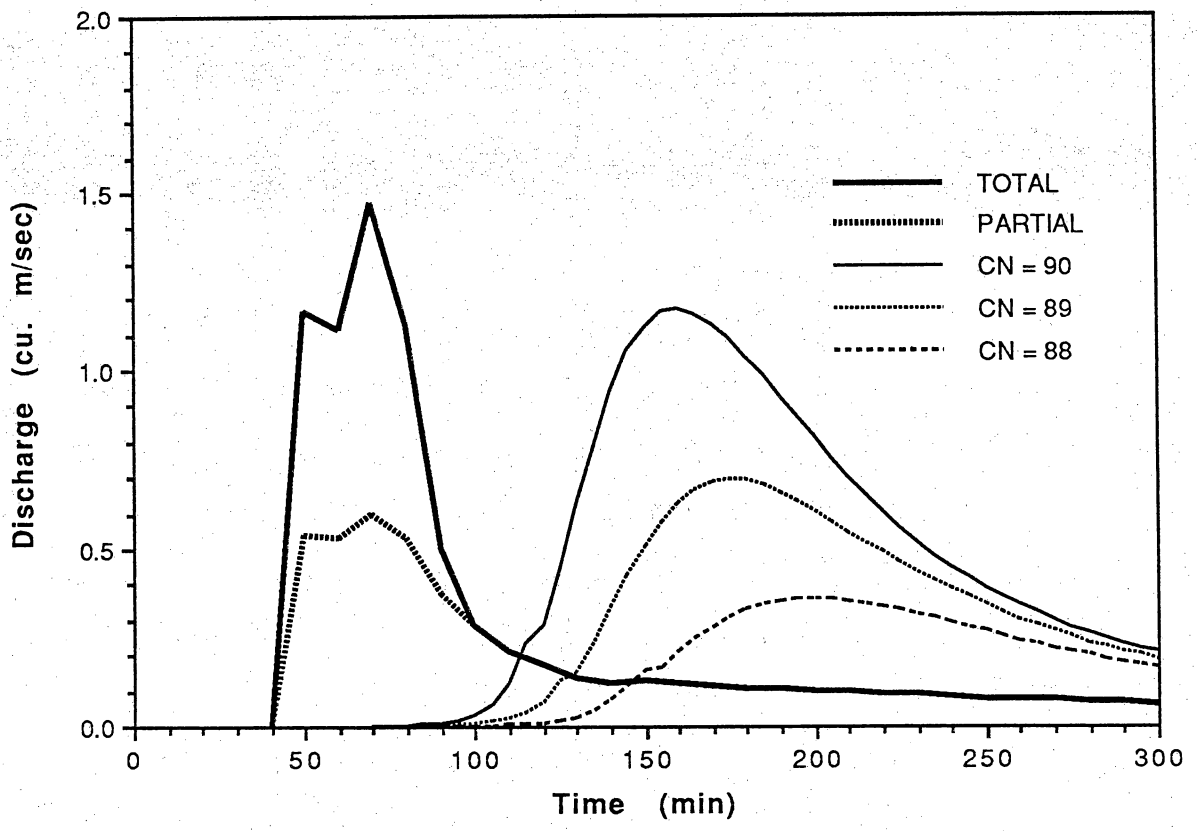

Figure 15. Hydrograph at gauging station 2 on 8-21-88 (kinematic routing model).

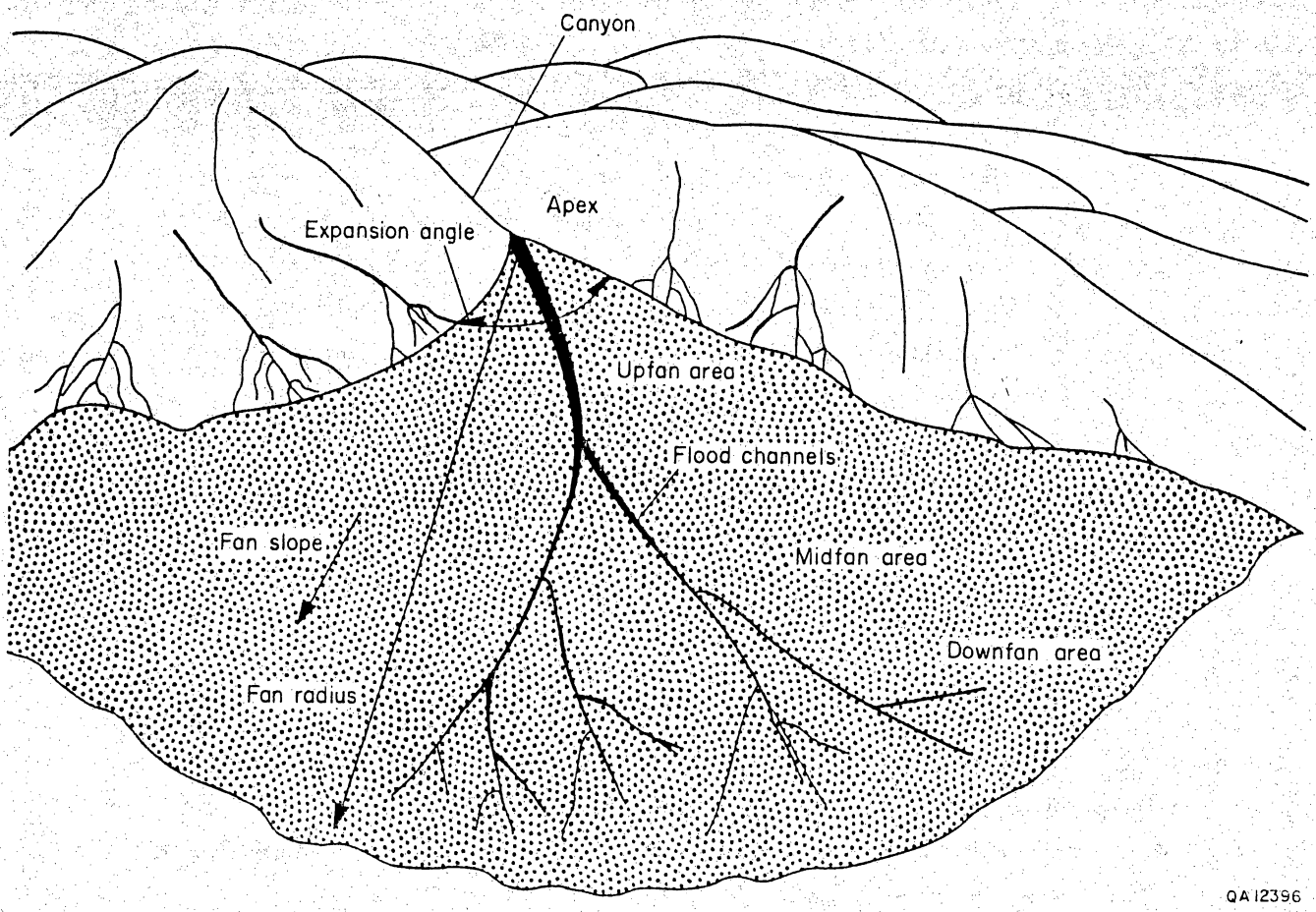

Figure 16. Definition sketch of alluvial fan characteristics.

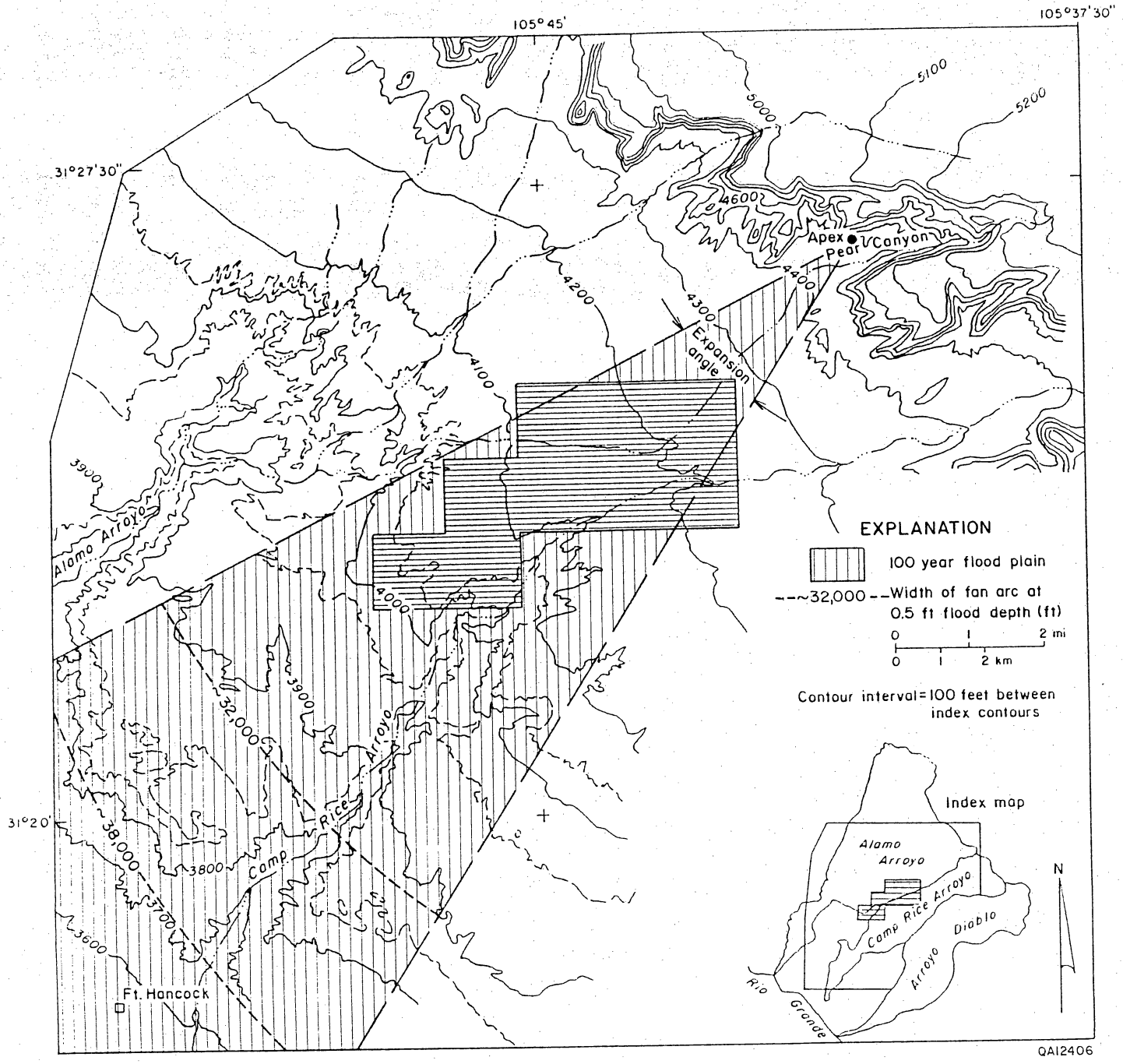

Figure 17. Flood profile for alluvial fan model in north part of study area.

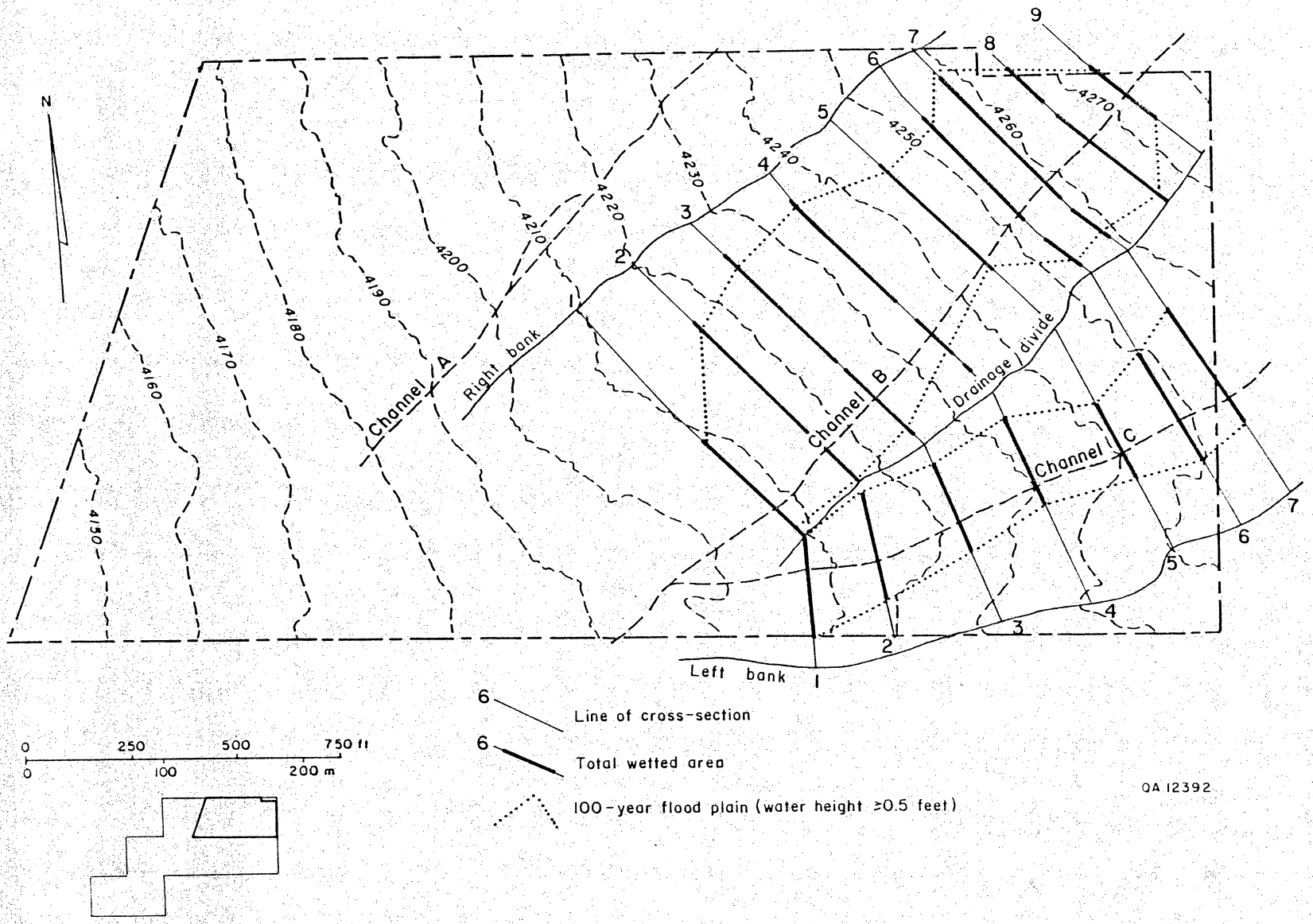

Figure 18. Flood profiles in two main channels in north part of the study area (watershed for lower fork of Alamo Arroyo).

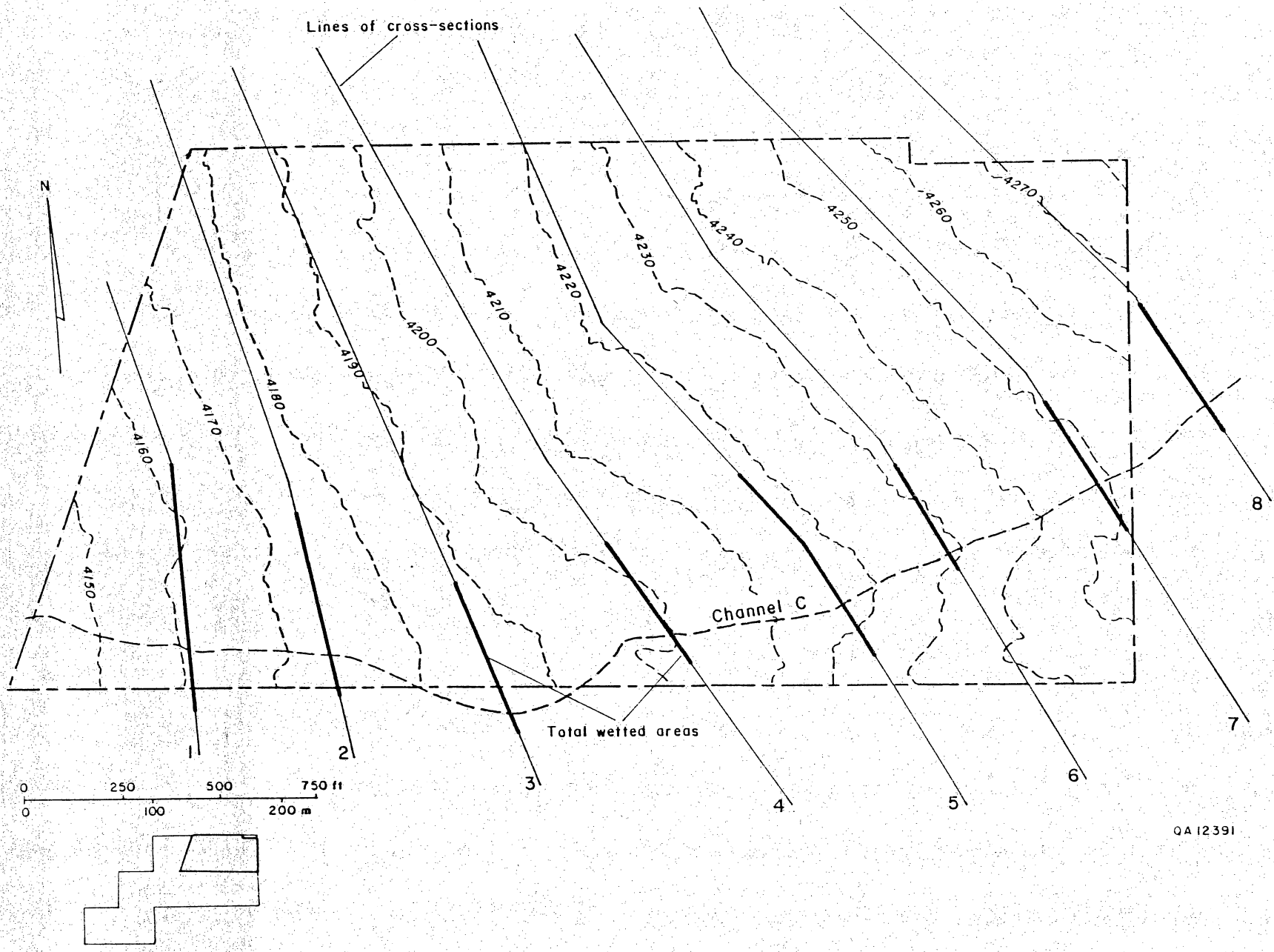

Figure 19. Flood profile in north part of study area. Channel C considered as single channel for the basin (watershed for lower fork of Alamo Arroyo).

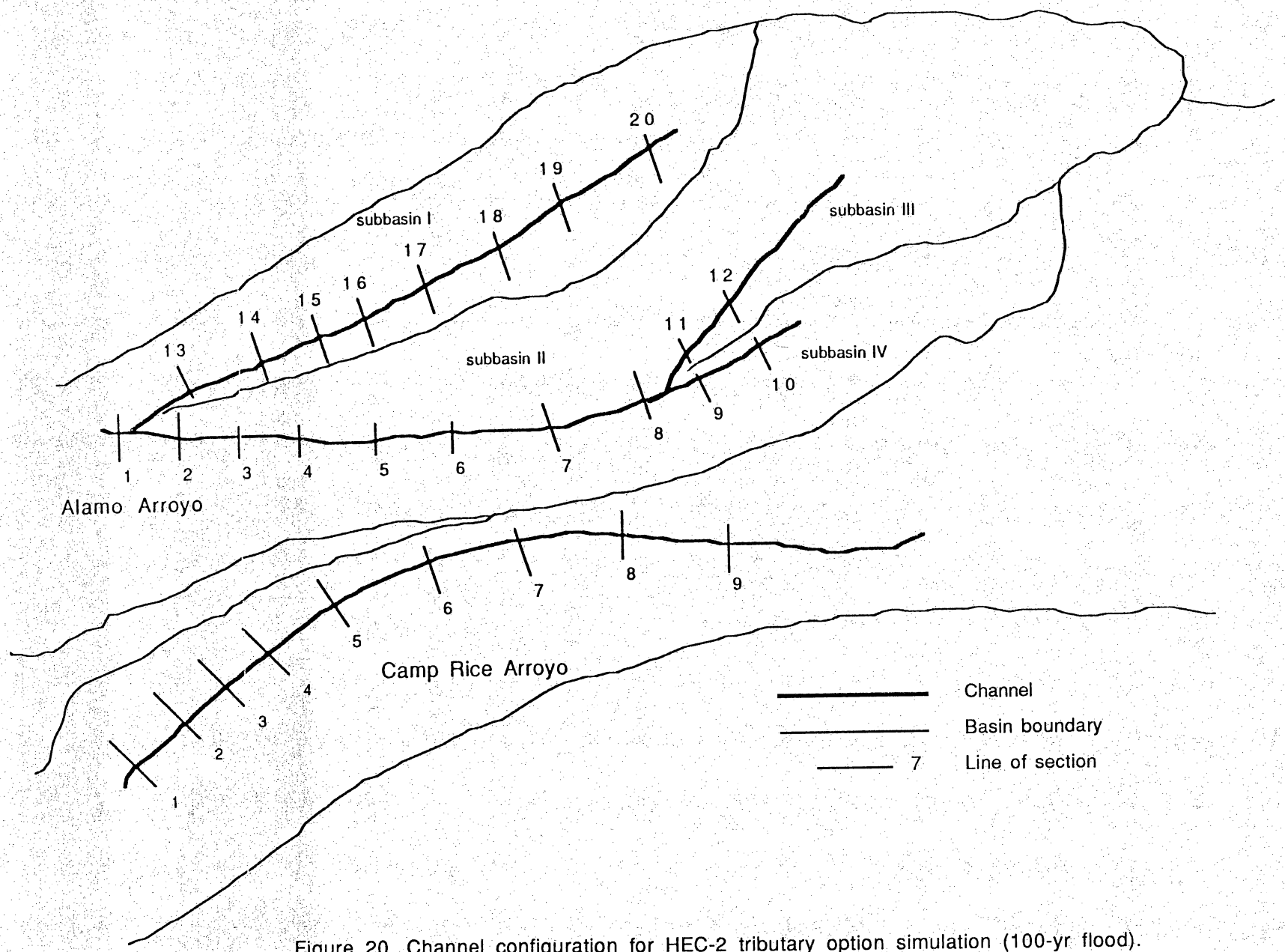

Figure 20. Channel configuration for HEC-2 tributary option simulation (100-yr flood).

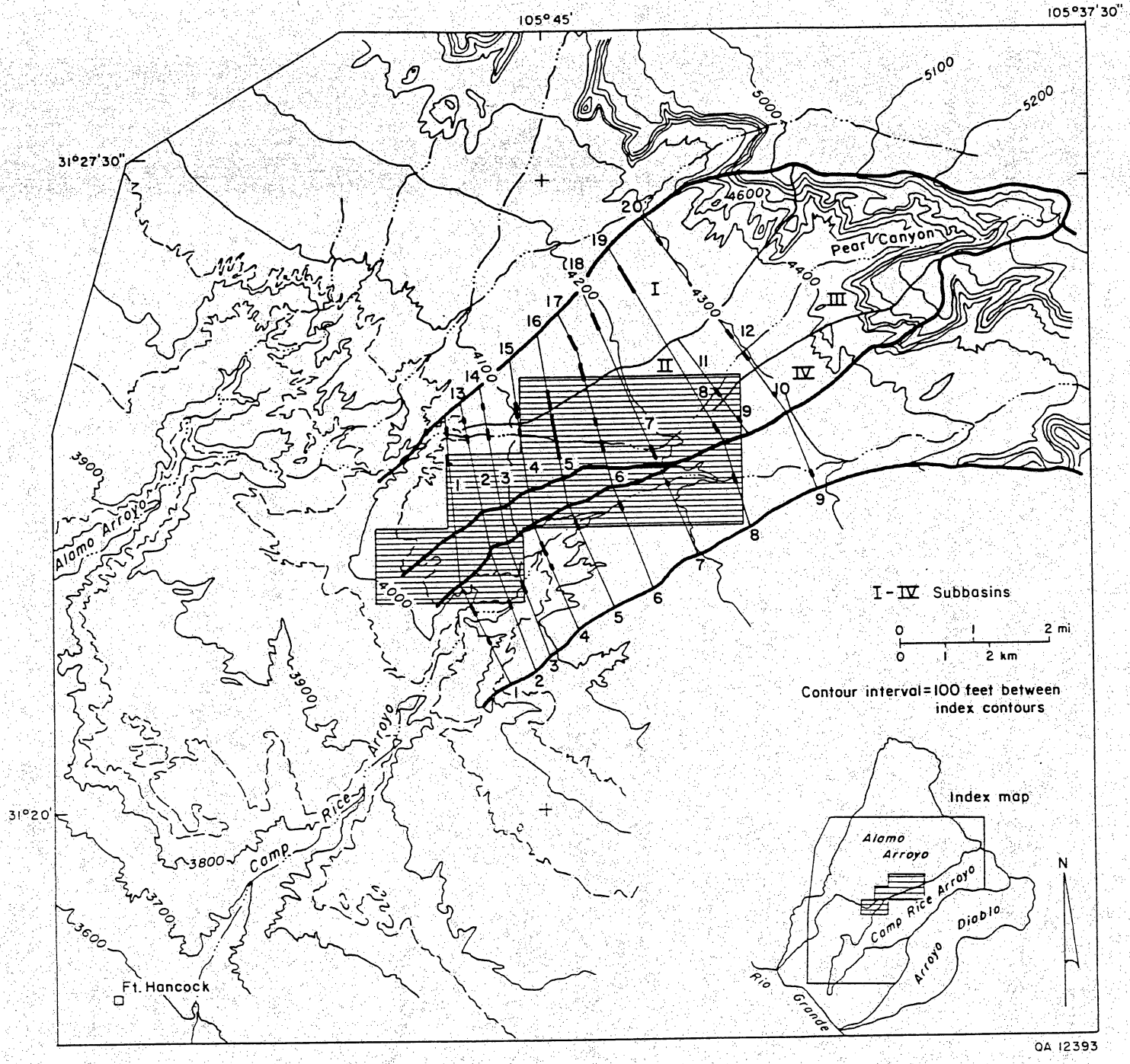

Figure 21. Flood profile for HEC-2 tributary option simulation (100-yr flood).

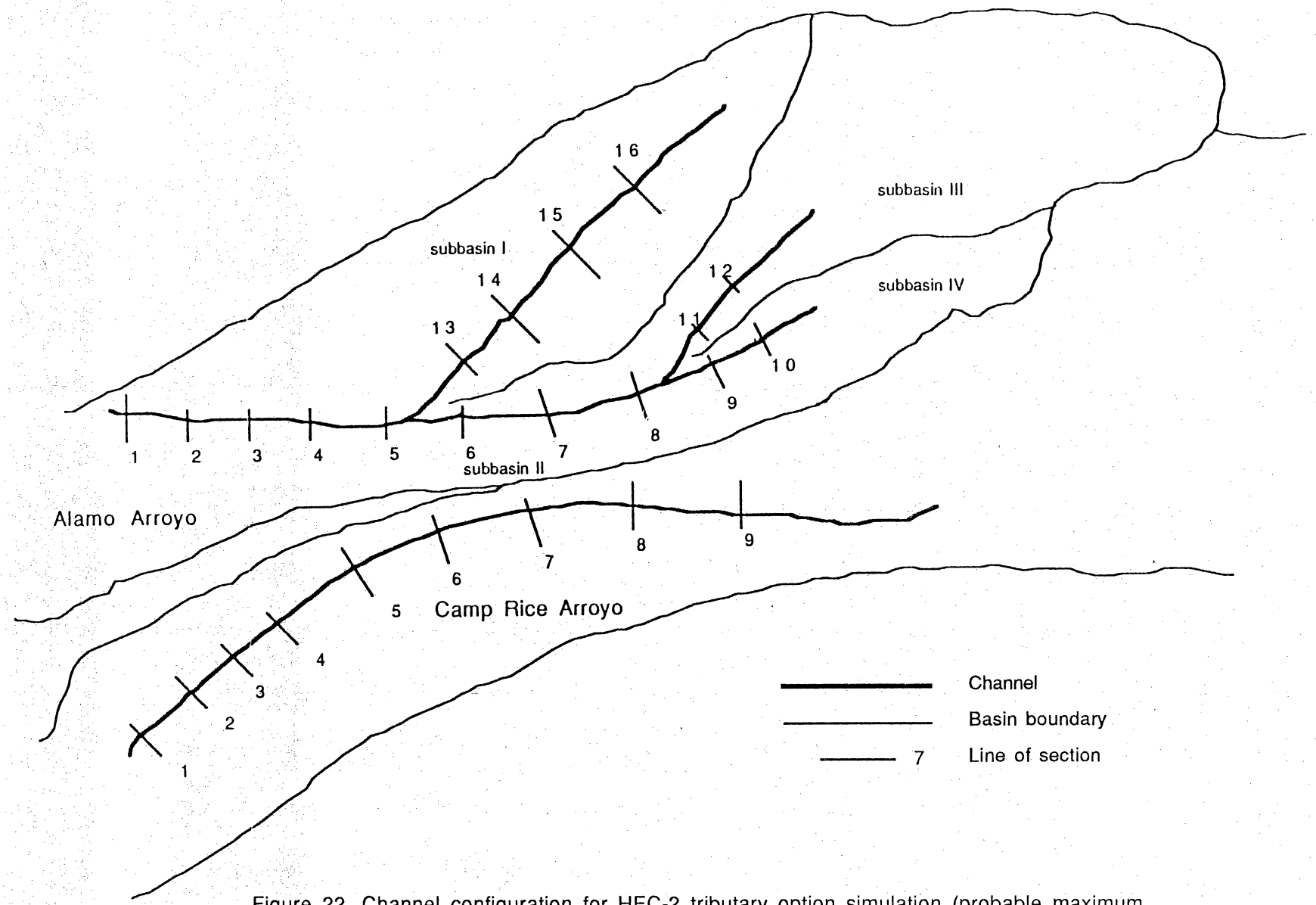

Figure 22. Channel configuration for HEC-2 tributary option simulation (probable maximum flood).

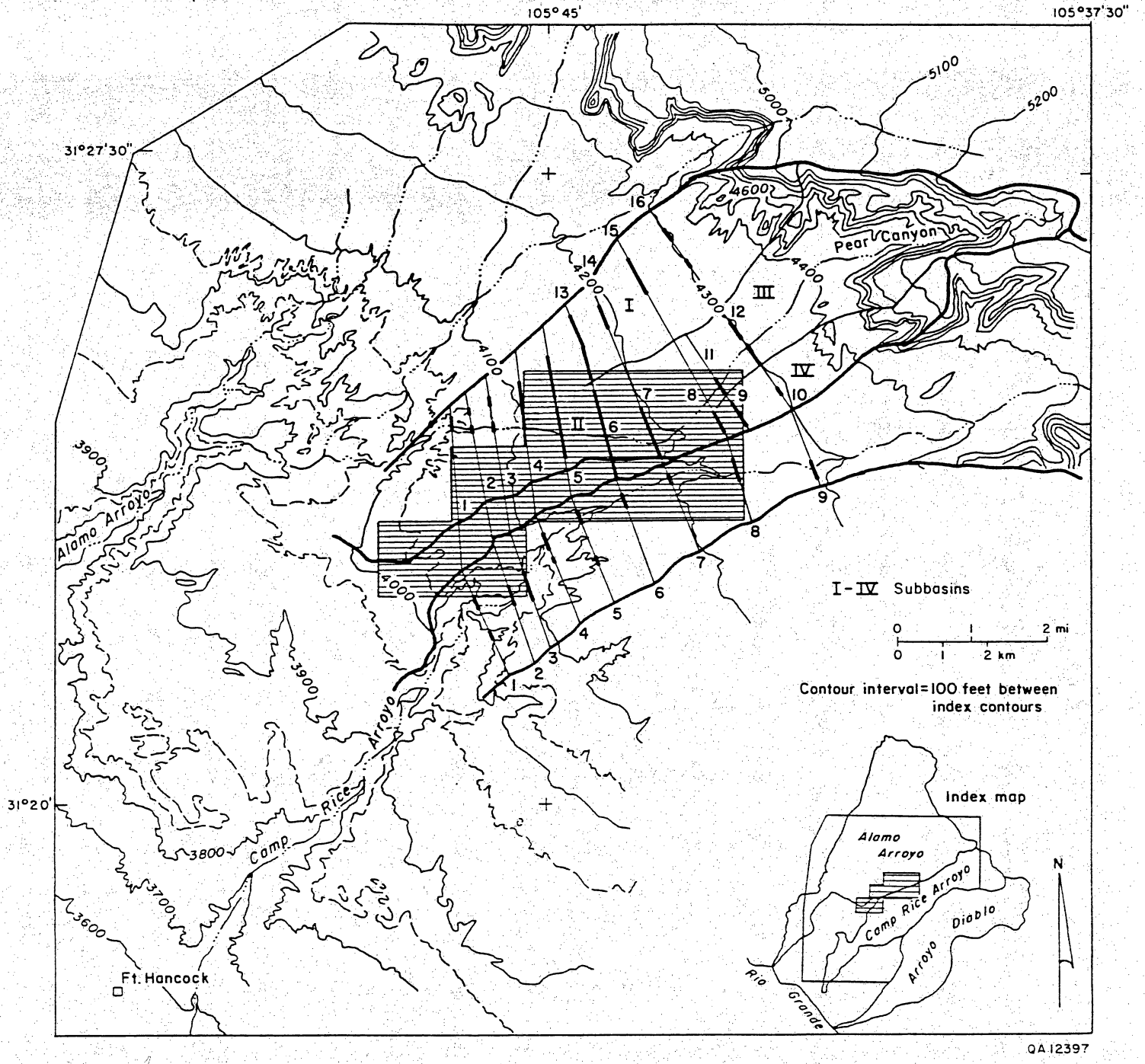

Figure 23. Flood profile for HEC-2 tributary option simulation (probable maximum flood).